Objective measurement of the navicular bursa volume in horses from low field magnetic resonance imaging (MRI) images using 3D Slicer® software

Marco Marcatili
DVM

Submitted in fulfilment of the requirements for the

Master Degree in Veterinary Medicine

School of Veterinary Medicine

College of Medical, Veterinary and Life Science (MVLS)

University of Glasgow November 2019

Abstract

Background: Navicular bursa (NB) effusion is considered a reaction of the structure to traumatic or degenerative processes. However, NB effusion can also be present in sound horses undergoing intense and regular exercise. To the best of the author's knowledge an objective non invasive method for measuring the NB volume has not been described to date. Accurate measurement of the NB volume using magnetic resonance imaging MRI would allow a more precise diagnosis and monitoring of response to treatment in horses with navicular bursitis.

Objectives: The overall objective was to validate an MRI based method for measuring NB volume in horses using 3D Slicer® software. This was achieved by two separate methodologies, *ex vivo* and clinical. During the *ex vivo* part of this study (Chapter 2 and 3) a method for measurement of the NB using MRI datasets was developed. During the clinical study (Chapter 4 and 5) the accuracy and precision of the method were calculated using MRI datasets.

The second objective of this study was to evaluate the performance of the current gold standard (subjective assessment by a board certified radiologist) against the newly developed method for cases with normal, mild, moderate and severe NB effusion (Chapter 5).

Hypothesis: The accuracy and precision of measurement of NB volume from MRI images in the horse using 3D Slicer® is sufficient for this method to be valuable in the investigation and management of lameness in clinical cases.

Material and methods: During the *ex-vivo* part of the study (Chapter 2) two forelimbs harvested from two adult thoroughbreds euthanised for reasons other than lameness were evaluated. The study design was approved by the Ethics and Welfare Committee of the School of Veterinary Medicine, University of Glasgow. An MRI-compatible needle was positioned in the NB and connected to a syringe. Water was injected in 1000 mm^3 increments up to a total of 3000 mm^3. Low field (0.31T, O-Scan equine®, Esaote Veterinary) sagittal T2 FSE and STIR MRI images were acquired before and after each injection. In order to visualise the landmarks for the NB boundaries 5000 mm^3 of contrast medium (2 mmol/L, Gadovist®) 2 mmol/L were injected into the bursa of an additional forelimb

prior to acquisition of T1 weighted sagittal MRI sequence. Volume was measured using 3D Slicer®.

In Chapter 3 the forelimbs of two adult thoroughbred euthanised for reasons unrelated to lameness were collected. The NB were each injected with water in 500 mm^3 increments until a total of 6000 mm^3 were injected. Sagittal T2 FSE MR sequences were acquired before the first injection and then after every injection. NB volume was measured by a single observer (intra-observer measurements) from the images using 3D Slicer® as described in Chapter 2. Three additional observers (two diplomates of the European College of Veterinary Surgeons and one diplomate of the American College of Veterinary Surgeons) performed volume measurements on NB injected with 1000, 1500, 2000 and 2500 mm3 in total (inter-observer measurements). The volume injected and volume measured were recorded in a spreadsheet (Excel®, Microsoft UK). Excel® was used to perform arithmetical calculations and statistical analyses, including plotting graphs, with the exception the Ryan-Joiner statistic for which Minitab® 19 was used (Minitab Ltd). Data were tested for normality using Ryan-Joiner statistic.

3D Slicer® was used to plan the treatment of a clinical case diagnosed with a deep digital flexor tendon (DDFT) core lesion (Chapter 4). The DDFT lesion was treated using intralesional injection of platelet rich plasma (PRP).

In chapter 5 twenty adult horses' front feet MRI studies acquired using a low field MRI scanner (0.31T, O-Scan equine®, Esaote Veterinary) were evaluated by a board certified radiologist who classified NB effusion as normal, mild, moderate or severe. NB volume was measured from sagittal T2 sequences using 3D Slicer® software. The ability of subjective measurements (current gold standard) to discriminate between groups was analysed using receiver operating characteristic (ROC) curves.

Results: The *ex-vivo* part of the study (Chapter 2) highlighted reduced underestimation of the NB measurements performed on T2 weighted images. However the variability of T2 weighted images was increased compared to STIR images. T2 weighted images were therefore used in the clinical parts of the study (Chapter 4 and 5). Intra-observer accuracy (difference between injected and

measured volume) was -40% (i.e. injected volume 1000 mm^3 measured volume 600 mm^3) over the range 500-6000 mm^3 (Chapter 3). The accuracy was improved (-27%) for lower volumes (500-3000 mm^3) (i.e. injected volume 1000 mm^3 measured volume 730 mm^3). Precision was similar for both volume ranges (28% and 30% respectively).

The inter-observer accuracy was 54% and precision 73%. One of the observers' measurements largely overestimated the NB volume. After these measurements were excluded the accuracy and precision were 32% and 69% respectively.

Measurement of the volume of the DDFT core lesion after PRP injection resulted in underestimation of the lesion volume by 30% compared to the volume injected (Chapter 4).

The results of the clinical study (Chapter 5) showed a statistically significant difference in the NB volume measured between NBs classified as having a normal or mild and severe degree of effusion. There was no statistically significant difference between moderate and all the other groups. A NB volume of 1768 mm^3 was able to distinguish between normal/mild navicular bursa volume and moderate/severe navicular bursa effusion with sensitivity and specificity of 90%.

Conclusion: The work presented supports the use of 3D Slicer® to objectively measure NB volume from sagittal T2w MR images in the horse. It also suggests that this method is superior to subjective assessment of NB volume. Objective measurement of NB volume may be helpful in indicating the presence of specific pathology (e.g. DDFT tear or fibrocartilage lesions), which may prompt further investigation and inform on best treatment and prognosis. Furthermore, the use of sequential measurement of synovial structures volume could be used to assess the response to the treatment.

Table of Contents

List of Tables

List of Figures

List of Accompanying Material

Peer reviewed abstracts presented at international conferences:

- Abstract presentation at the 26th ECVS Annual Scientific Meeting 13-15th July in Edinburgh, Scotland.

  AUTHORS: M. Marcatili, J. Marshall and L. Voute

  TITLE: Accuracy and precision of equine navicular bursa volume measurement made from low field MRI datasets using 3D Slicer® software – an *ex-vivo* study.

  (Appendix 1)

- Abstract presentation at the BEVA congress in Birmingham 12-15th September 2018.

  AUTHORS: M. Marcatili, J. Marshall, A. McKnight and L. Voute

  TITLE: Objective measurement of navicular bursa volume.

  (Appendix 2)

- Consent form signed by the owners of the horses enrolled in the clinical study. (Appendix 3)

- MRI sequences technical parameters

  (Appendix 4)

Acknowledgement

Firstly, I would like to thank my primary supervisors Dr Lance Voute, Dr Jonathan Withers and co-supervisor Dr John Marshall for the constant support provided throughout the study design and related research. Completion of this project without their help, support and guidance would have not been possible. I would also like to thank Professor Sandy Love for his help during the residency. A big thank you goes to Dr. Alexia McNight for the help and expertise provided thoughout the masters program.

I would like to thank my parents and my sister for the support they have shown throughout. A big thank you goes to Federica for being so patient and always very supportive before and during my residency.

I would also like to thank all the colleagues and support staff of the Weipers Centre Equine Hospital David, Derek, Etienne, Yasmin, Tracy, Anna, Lynsey, Lenka, Lyndsay, Mary, Victoria Elspeth to make my stay at the Weipers a real pleasure.

I thank all my fellow current and past residents at the Weipers Christian, Sarah, Lauren, Alex, Francina and Andrea for the nice moments we have had in the last 4 years.

A thank you goes to my colleagues at Pool House Equine Clinic Richard, Gil, Patrick, Sam and Ronald who always supported me during the time spent working at the clinic.

Author’s Declaration

“I declare that, except where explicit reference is made to the contribution of others, that this dissertation is the result of my own work and has not been submitted for any other degree at the University of Glasgow or any other institution.”

Printed Name: Marco Marcatili

Signature: _____

Ethical approval

The study design was approved by the Ethics and Welfare Committee of the School of Veterinary Medicine, University of Glasgow.

Consent was given by owners for the use of their horse's limbs (Chapters 2 and 3) or images (Chapters 4 and 5). The form used for this purpose is shown in Appendix 3.

Definitions/Abbreviations

- AAEP: American Association Equine Practitioners
- ACVR: American College of Veterinary Radiology
- ACVS: American College of Veterinary Surgeons
- ANOVA: Analysis of Variance
- CE: Contrast Enhanced
- CT: Computer Tomography
- DDFT: Deep Digital Flexor Tendon
- DFTS: Digital Flexor Tendon Sheath
- DICOM: Digital Imaging and Communications in Medicine
- DIPJ: Distal Interphalangeal Joint
- DVM: Doctor Veterinary Medicine
- ECVS: European College of Veterinary Surgeons
- LF: Left Forelimb
- MR: Magnetic Resonance
- MRI: Magnetic Resonance Imaging
- NB: Navicular Bursa
- NSAIDs: Nonsteroidal anti-inflammatory drugs

- OA: Osteoarthritis
- PD: Proton density
- PET: Positron Emission Tomography
- RF: Right Forelimb
- ROC: Receiver Operating Characteristic
- SD: Standard Deviation
- SF: Synovial fluid
- STIR: Short-Tau Inversion Recovery
- STV: Synovial Tissue Volume
- WORMS: Whole-Organ Magnetic Resonance Imaging Score

1 Literature review

1.1 Introduction

1.1.1 Why is it useful to measure navicular bursa volume in the horse?

Effusion of synovial joints and bursae is considered a reaction of the structure to traumatic or degenerative processes (Ross 2011). However, synovial effusion can also be present in sound horses undergoing intense and regular exercise (e.g. affecting the fetlock and tarsocrural joints) (Ross 2011). For this reason measurement and establishment of a 'normal' degree of effusion has been a target of research for many years (Ekman *et al* 1981).

The foot is the most common source of pain in horses presented with lameness (Ross 2011). Several structures may be involved either singly or in combination. The deep digital flexor tendon (DDFT) alone can be injured in up to in 59% of the cases in which lameness is localised to the foot. Injury of DDFT, navicular bone and collateral ligaments of the distal interphalangeal joint (DIPJ) are detected in 31% of the cases. Furthermore, effusion of the NB (navicular bursa) is diagnosed in 44% of the cases (Sampson *et al* 2009).

The advent of new imaging modalities, namely magnetic resonance imaging (MRI) and computed tomography (CT), has permitted three dimensional imaging of synovial structures within the horse's foot (i.e. NB and DPIJ). Effusion of the NB is relatively commonly identified in MR studies but establishing the clinical significance of this can be difficult, especially if it is an isolated finding. Navicular bursa effusion is currently evaluated subjectively by estimating the size of the fluid signal between the DDFT and collateral sesamoidean ligament and the signal representing the abaxial proximal bursal outpouchings (Sampson *et al* 2009). However, the use of a subjective method may limit the accuracy and precision of assessment. Furthermore, the 'normal' range for effusion of the NB has not been described and therefore judgement relating to significance is likely to be influenced by the observer's experience. A method for objective measurement of synovial structure volume should allow more accurate and precise evaluation, and inform the differentiation between 'normal' and 'abnormal' effusion. A validated, objective method of synovial volume measurement would also allow comparison between

different time points and so inform judgement about the clinical progress of cases where MRI is available.

1.1.2 Navicular bursa anatomy

The navicular bursa (NB) together with the distal interphalangeal joint (DIPJ) are the main synovial structures assessed during MRI examination of the equine foot. Whilst subjective evaluation of the degree of effusion of the DIPJ is sometimes possible through palpation of the dorsal recess, assessment of NB effusion cannot be performed similarly because the NB is entirely enclosed within the hoof capsule. Its dorsal border is demarcated, from proximal to distal, by the navicular suspensory ligament and the “T” ligament, palmar/plantar fibrocartilage of the navicular bone and distal sesamoidean impar ligament. Palmarly/plantarly the dorsal aspect of the deep digital flexor tendon (DDFT) contours the NB as it runs to its insertion into the distal phalanx. Palmar and abaxial to the DDFT the NB expands into two palmar/plantar pouches. Proximally the NB is separated from the digital flexor tendon sheath (DFTS) by the “T” ligament (McIlwraith 2015). The NB volume based on the volume of contrast medium injected has previously been reported to be 3000mm^3 (Turner 1998).

1.1.3 Inflammation of the navicular bursa

Inflammation of the NB, otherwise known as podotrochlear bursitis or bursitis of the NB, is characterised by fluid distension of the NB with or without proliferation of soft tissues (Coelho and Kinns 2012). Fluid distension of the NB it is seen as high signal intensity on T2, PD and STIR MR images. Currently distension of the NB is considered within normal limits when only a small amount of fluid is seen in the proximal palmar/plantar pouches (Sampson *et al* 2009). Due to the anatomy of the NB and compression by the adjacent deep digital flexor tendon (DDFT), fluid is rarely seen collected between the navicular bone and the DDFT unless the distension is marked (when it can be identified as a thin line between these structures). In some cases the increased effusion of the NB results in fluid pooling

at the level of the mid-sagittal ridge synovial fossa (Schramme et al 2009). This is considered a normal finding.

The prevalence and aetiology of primary bursitis of the NB is not known, nor is its relationship to the development of navicular disease (Dyson *et al* 2011). When horses with navicular disease were compared to normal horses, the navicular disease group presented with villous hypertrophy, hyperplasia of lining cells and venous congestion of the synovium of the bursa (Svalastoga *et al* 1983). More recent studies reported no evidence of acute inflammation of the NB in horses with palmar foot pain or in age-matched controls (Dyson *et al* 2006); however, lame horses had greater synovial proliferation compared to controls (Murray *et al* 2006; Blunden *et al* 2006).

1.1.4 Investigation and treatment of navicular bursitis

Ultrasonographic examination of the NB (using a 7.5 MHz curvilinear transducer) enables visualisation of the palmar pouches as far distally as the proximal margin of the navicular bone (Carstens and Smith 2014). This method uses a small imaging window in the distal pastern region between the heel bulbs and a small footprint transducer (normally curvilinear). The foot is placed on a wedge, which partially flexes the distal limb. In some breeds (i.e. Cob) the thickness of the skin affects image quality to the extent that it is non-diagnostic. A transcuneal approach has also been described which allows visualization of the most distal portion of the DDFT and navicular bursal recess (Busoni and Denoix 2001). Before performing transcuneal ultrasonography the frog should be trimmed to produce a smooth surface for the transducer. The foot is then soaked in a poultice for at least one hour to increase hydration of the frog horn but in some cases an overnight soak may be needed. After the initial preparation acoustic coupling gel is applied in order to fill the central sulcus of the frog and reduce artefact formation. The leg is then held in flexion and the ultrasonographic examination is performed through the central cuneal sulcus and body of the frog. Ultrasonographic images are then acquired in a sagittal or parasagittal plane and the transverse plane. The usefulness of ultrasound for evaluation of the NB volume is questionable due to

limited visualisation resulting from anatomical, technical and patient related factors.

Contrast enhanced computer tomography has also been used to evaluate soft tissue lesions within the foot (Vallace et al 2012, van Hamel et al 2014). However, the identification of synovial structures was shown to be improved by for low field MRI (Vallace et al 2012).

For the above mentioned reasons magnetic resonance imaging is the modality of choice for assessing soft tissue structures within the equine digit (Maher *et al* 2011). A common indication for MRI would be foot pain which is not accompanied by significant radiographic findings. This modality has largely replaced the use of ultrasonography.

When horses with a recent onset of clinical signs of navicular syndrome (without any radiographic abnormalities) were examined using MRI, 44% had increased synovial fluid in the NB (Sampson *et al* 2009). However, in the same study a small increase in the volume of fluid was found in most of the horses. Twenty-nine percent of horses were considered to have severe fluid distension and 71% of these had a deep digital flexor tendon (DDFT) lesion at the level of the NB.

Although it appears that distension of the NB is a common MRI finding in horses with foot pain (Dyson *et al* 2005; Sampson *et al* 2009) to our knowledge there is currently no agreement on what the cut-off to distinguish ‘normal’ from ‘abnormal’ should be.

In the last decade the use of navicular bursoscopy for the treatment of dorsal border DDFT tears within the NB and adhesions between the DDFT and the fibrocartilage of the navicular bone has increased (Smith *et al* 2007; Smith *et al* 2012). The surgery is performed under general anaesthesia, with a transthecal approach being preferred because it provides better access that the direct approach (McIlwraith *et al* 2015). The arthroscope is inserted in the digital flexor tendon sheath dorsal to the dorsal border of the DDFT at the level of the proximal interphalangeal joint. The NB is entered through dissection of the T ligament using a sharp instrument (i.e. fixed blade meniscectomy knife). This approach allows

examination of the proximal two thirds of the NB where DDFT lesions and adhesions are most commonly identified (Sampson *et al* 2009).

A direct bursoscopic approach to the NB has also been described (Wright et al 1999). This approach allows advancement of the arthroscope to the most distal portions of the NB including the impar ligament. This approach is also considered the ideal approach for treatment of sepsis of the NB. Furthermore, the use of an alternate approach has been reported to reduce the risk of penetration of other synovial structures (i.e. DIPJ and DFTS) (Kane-Smith et al 2016).

1.1.5 Methods used to measure synovial volume

Synovial volume measurement is considered an important parameter for both diagnosis and monitoring response to treatment in human medicine. The majority of the studies in this subject area have been conducted on human knees affected by osteoarthritis (OA). One of the first approaches to synovial fluid volume estimation was based on radioisotopic dilution, involving [113In]-indium chloride or sodium [99Tc]-pertechnetate (Rekonen *et al* 1973). Geborek *et al* (1988) described a non-radioactive method for estimating intra-articular volume based on albumin dilution after intra-articular injection of saline. This method required aspiration of an initial volume of synovial fluid. The volume of the fluid still present within the joint was calculated by injecting a known quantity of saline solution followed by 2 minutes of external joint massage and subsequent resampling of the joint. The residual volume was calculated by comparing the concentration of albumin before and after dilution.

Another reported method of measuring synovial fluid volume based on dilution techniques, which was tested in rabbits, relied upon injection of high molecular weight dextrans (fluorescently tagged) in order to minimize potential efflux of marker from the joint after intra-articular injection (Delecrin and Oka 1992). The original synovial fluid volume was calculated using the fluorescence intensities of the injected and retrieved synovial fluid.

In 1989 the use of imaging methods for the measurement of the volume of synovial structures in human medicine was introduced. Three-dimensional processing of CT or MRI images was investigated (Heuck *et al* 1989) in a study which concluded that measurements based on MR images were more accurate than those based on CT images.

Clinical application of MRI for the measurement of synovial structures volume in people was evaluated for the first time in 1994 (Ostergaard *et al* 1994). The authors used gadolinium enhanced transverse T1-weighted images to calculate synovial fluid volume, identifying a high correlation between actual volume and measured volume. They therefore suggested that this method had a role in the assessment of disease severity and response to treatment - the accuracy of synovial fluid volume measurement using this method was reported to be 20% (Ostergaard *et al* 1995). The use of contrast enhanced MRI to assess the response to intra-articular medication with corticosteroids in clinical cases was investigated in a separate study (Ostergaard *et al* 1996), with the authors concluding that synovial volume measurement was reproducible and further that pre-treatment synovial volume may have predictive value for the treatment of rheumatoid arthritis in people (Ostergaard *et al* 1996).

More recent studies in laboratory animals estimated synovial fluid volume by dividing the total calcium concentration in joint cavity lavage fluid by plasma calcium concentration (Matsuzaka *et al* 2002). The method was validated calculating the radioactivity in plasma and joint lavage fluid after intravenous injection of $^{3}H_2O$. A statistically significant correlation was observed between the values obtained with the two methods. One of the advantages of this method is that it relies upon a native molecule, however, changes in the concentration of calcium can occur in relation to different cells' activity. A method for the measurement of synovial fluid volume using urea concentration in synovial fluid and in serum has also been described (Kraus *et al* 2007). For this method a serum sample is collected just before arthrocentesis is performed and a synovial sample was collected either directly and by lavage. Synovial volume is then calculated with the formula shown in Figure 1.0.

$$Vj = CD(VI)/(C-CD)$$

Figure 1.1. Vj = volume of synovial fluid (SF) in entire joint; CD = urea concentration in diluted sample (lavage) SF; VI=volume saline injected into joint; C = urea concentration in undiluted (neat) SF.

The constant SF/serum urea ratio of 0.897 (regardless of disease severity, inflammation or animal age) makes it possible to calculate intra articular volume of joints based upon the method, as well as conferring an advantage over the previously described method using calcium. In fact, measurement of synovial fluid volume based on calcium concentration can only be employed when the patient is not receiving non-steroidal anti-inflammatory drugs (NSAIDs) or other drugs with calcium as a counter ion. This avoids interference with the concentration of calcium in the synovial fluid or plasma.

In 2010 a fully automated system for the quantification of human joint effusion from MR images was validated (Li *et al* 2010). In this study, high field MRI (1.5 T) T1- and T2-weighted sequences were used. The measurements, which were performed on phantoms based on regular cylindrical or spherical shapes the measurements were found to have a very small coefficient of variation (0.8-1.4%). More recently, semiquantitative MRI with or without contrast enhanced sequences (CE) has been used to evaluate synovial membrane inflammation and joint effusion in human patients affected by knee OA (Loeuille 2011). T1-weighted CE images were acquired after intrasynovial injection of 0.1 mmol/kg of gadolinium contrast medium. Synovial distension was evaluated with two different semiquantitative scales. The WORMS (Whole-Organ Magnetic Resonance Imaging Score) (Peterfy *et al* 2004) was used for axial T2w images whereas the MRI-effusion score was used for T1w CE images.

When WORMS (T2w images) was used, synovial membrane thickening and joint distension were graded together on a scale that varied from 0 to 3 in terms of the estimated maximal distension of the synovial cavity: 0 = normal; grade 1 = <33% of maximum potential distension; grade 2 = 33-66% of maximum potential distension; and grade 3 = >66% of maximum potential distension. For the MRI-effusion score (T1w CE images), only low signal intensity within the intra articular

cavity distinct from the enhancing synovium was scored on an axial CE sequences in the suprapatellar pouch, 1 cm above the patella, and in the lateral and medial recesses at the level of the centre of the patella. A four-point scale was used: grade 0 = no distension; grade 1 = minimal distension; grade 2 = moderate distension; grade 3 = major distension defined by capsular distension. The distension score was the sum of the scores for the three compartments of the knee and varied from 0 = absence of distension, to 9 = severe distension. The results of this study showed that joint effusion can be assessed with the same level of performance on T2w and T1w CE images on MRI. However, the contrast enhanced T1w CE images were more accurate in assessing the impact of synovial inflammation and especially cellular infiltration. A moderate correlation between joint volume measurements based on arthrocentesis and MRI measurements was also found. However, the exact volume of fluid was not calculated from MRI images.

O'Neill and colleagues (2016) recently published a study describing the use of MRI to monitor the effect of treatment of knee OA in the human by intra-articular medication. The synovial tissue volume (STV) was calculated on T1w FS post CE MRI images. The post-CE images were manually segmented (i.e. partitioned in regions of interest so that each region corresponded to one or more anatomical structures) and using computer image analysis the cartilage was excluded by thresholding within the segments. The rest of the segmented space was assumed to be a mixture of synovial fluid and synovial tissue. The proportion of synovial tissue was calculated in every voxel ($P=(I-mf)/(ms-mf)$) truncated to [0, 1], where I is the voxel intensity, and m_f and m_s are the means of the intensity distributions of fluid and STV, respectively. Using the above mentioned equation, it was possible to calculate the synovial fluid volume. The main disadvantage of this method is the requirement for CE images.

Radioisotopic dilution methods, albumin dilution, injection of high molecular weight dextrans and methods measuring the calcium concentration are not currently used in any clinical setting (human or veterinary). Joint volume measurement based on urea concentration in synovial fluid and serum is used in equine practice (Gough et al 2002). However, the advent of MR imaging based methods for synovial volume measurement offers a valuable alternative, especially where obtaining a synovial fluid sample is technically challenging (for example, the navicular bursa)

and when additional diagnostic information would contribute usefully to case management.

1.1.6 3D Slicer®

3D Slicer® is a free open-source software program used for visualization and analysis of medical images (www.slicer.org). This cross platform program is made up of modules and layers providing a closed circuit interface with a library and toolkit (Pieper *et al* 2007). Upload of DICOM files allows reading of computer tomography (CT), positron emission tomography (PET) and MRI data sets in both 2D and 3D. Once the files have been uploaded, image slices can be viewed with user determined orientations and settings. The program is provided with a number of different core modules such as: volume measurement, registration and editor. Once a module has been chosen it is possible to select one of the subcategories (e.g. paint tool, erase, draw etc) in order to carry out more specific tasks using the linked functions. The broad range of functionality offered by 3D Slicer® has been utilised in biomedical research and in the study of the brain in particular. The application has facilitated the description of normal brain structure (Li *et al* 2010) and the investigation of brain diseases, such as tumours (Egger *et al* 2013; Jennings *et al* 2013; Mercea 1985) and autism (Wolff *et al* 2012). A preliminary study of 3D Slicer®'s potential as a diagnostic tool in the veterinary field was performed in 2014 at the University of Glasgow. The findings of this study indicated that 3D Slicer® could detect an increase in volume of the distal interphalangeal joint of horses in MR images when the joint was injected with fluid (Prior 2014). This preliminary work and the versatility of 3D Slicer® made it the ideal application for use in the present study.

The overall aim of this study was to validate an objective MRI based method for the measurement of the navicular bursa (NB) volume. The work has been divided into two chapters:

- **Chapter 2 – *Ex-vivo* study**: To develop a method for measurement of equine navicular bursa volume using the combination of MR imaging and image processing performed post-acquisition.

- **Chapter 3 – *Ex-vivo* study:** To obtain data on the accuracy and precision of measurement of equine navicular bursa volume by post-acquisition processing of T2 sequence MR images using 3D Slicer® (the method described in Chapter 2).

1.2 Hypothesis

The overall hypothesis for the project was: the accuracy and precision of measurement of NB volume from MR images in the horse using 3D Slicer® is sufficient for this method to be valuable in the investigation of lameness in clinical cases.

The hypothesis was tested in subsequent steps:

- Ex-vivo study: Chapter 2 focussed on establishing the method, providing the groundwork for the hypothesis to be tested in the experiment performed in Chapter 3 (Validation of measurement of equine navicular bursa volume using low field MRI datasets and 3D Slicer® software).

- Clinical study: The applicability of the methodwas explored through application of the method to clinical cases (Chapter 4: Use of 3D Slicer® platform as planning and intraoperative aid in the management of a clinical case affected by deep digital flexor tendon (DDFT) core lesion; Chapter 5: Use of 3D Slicer® for the measurement of the navicular bursa volume in clinical cases).

2 Measurement of equine navicular bursa volume using low field MRI datasets and 3D Slicer® software – development of the method

2.1 Introduction

Measurement of the volume of synovial cavities has been a subject of research for many years. Assessment of the response to treatment, joint health and correlation between joint volume and pain are the main reasons for this interest. Recent confirmation of a positive association between degree of synovial effusion and pain (O'Neill *et al* 2016) has stimulated research interest in the field further. The early methods for synovial volume measurement described include: radioisotopic dilution (Rekonen *et al* 1973), non-radioactive methods based on albumin dilution after intra-articular injection of saline (Geborek *et al* 1988) or injection of high molecular weight dextrans (Delecrin *et al* 1992). In 1989 the use of imaging methods for the measurement of the volume of synovial structures was introduced for the first time in human medicine. Heuck and colleagues (1989) investigated the use of three-dimensional processing of CT or MRI images. This study concluded that quantification of synovial fluid volume with three-dimensional data processing offers more accuracy when using MR images compared to CT images. The clinical application of MRI-based synovial fluid volume measurement was assessed for the first time in 1994 (Ostergaard *et al* 1994). The authors used gadolinium enhanced transverse T1-weighted images to calculate synovial fluid volume, identifying a strong correlation between actual and measured volume. They therefore suggested that this method had a role in the assessment of disease severity and response to treatment - the accuracy of synovial fluid volume measurement using this method was reported to be 20% (Ostergaard *et al* 1995). The use of contrast enhanced MRI to assess the response to intra-articular medication with corticosteroids in clinical cases was investigated in a separate study, with the authors concluding that synovial volume measurement was reproducible and that pre-treatment synovial volume may have predictive value for rheumatoid arthritis outcome in people (Ostergaard *et al* 1996). More recently the ratio of calcium concentration within a joint and serum calcium concentration was used to determine synovial fluid volume (Matsuzaka *et al* 2002). One of the flaws of this method is the effect of different drugs (i.e. NSAIDs) on calcium concentration and therefore volume measurement. In 2007 Kraus *et al* described a

method for volume measurement based on the ratio of urea concentrations in synovial fluid and serum. This ratio was found to be constant and not influenced by disease severity, inflammation (cell count) or age. However, the method requires synoviocentesis to be performed (Kraus *et al* 2007). In 2010 a fully automated system for the quantification of human joint effusion from MR images was validated (Li *et al* 2010). In this study high field MRI (1.5 T) T1- and T2-weighted sequences were used. The measurements, which were performed on phantoms based on regular cylindrical or spherical shapes, were found to have a very small coefficient of variation (0.8-1.4%). More recently the use of semi-quantitative MRI with or without contrast enhancement has replaced the use of more invasive methods for the assessment of joint effusion and synovial membrane inflammation in human patients affected by knee OA (Loeuille 2011).

To date there are no guidelines to objectively estimate the volume of synovial structures within the foot. A preliminary study has investigated the ability to objectively measure the volume of the equine dital interphalangeal joint (DIPJ) (Prior and Marshall 2014). However, the navicular bursa (NB) represents a unique challenge due to its anatomical location (i.e. completely enclosed in the hoof capsule). The anatomical location of the navicular bursa (NB) precludes clinical assessment of its degree of effusion. The usefulness of ultrasound for evaluation of the NB volume is questionable due to limited visualisation resulting from anatomical, technical and patient related factors. The use of methods based on synovial fluid analysis (i.e. calcium or urea based) require collection of synovial fluid which. This procedure is often performed with the horse sedated and with the distal limb anesthetised. Furthermore, collection of synovial fluid sample can be challenging particularly in those cases with minimal NB effusion of adhesion formation. For these reasons the use of a non invasive imaging method for the measurement of the NB volume is considered advantageous.

2.2 Aim

The work described in this chapter aimed to develop a method for measurement of equine navicular bursa volume using the combination of MR imaging and image processing performed post-acquisition.

2.3 Objectives

The objectives for the work were to:

1. Establish a method for the measurement of navicular bursa volume from MRI datasets using 3D Slicer® (www.slicer.org).

2. Obtain preliminary data for how the method performs.

2.4 Materials and methods

2.4.1 Specimen preparation

Distal forelimbs harvested from adult Thoroughbred horses euthanized for reasons other than forelimb lameness and without a history of pathology of the podotrochlear apparatus were used in the work described in this chapter. The limbs were stored a 4°C for a maximum of 36 hours and brought up to room temperature prior to use. Limbs were not batched by storing them at -20°C because of concerns about the adverse effects of thawing on navicular bursa (NB) integrity and about the potential for reduction in image quality or needle (soft alloy) bending or breakage due to incomplete thawing.

For NB injections, a 20 G 10 cm MRI compatible needle (MRI Chiba Needle, Somatex®) was inserted into the NB using a palmar midline approach (Schramme *et al* 2006). Needle positioning was confirmed with a lateromedial radiograph. Acquisition of the lateromedial radiograph also allowed identification of metal within the hoof capsule (nail remnants) that result in artefact formation during imaging. In cases where metallic material was identified further radiographic views were taken in order to guide its removal. During needle positioning particular care was paid to avoid multiple penetrations of the NB to minimise leakage from the NB when distended. Once correctly positioned, the needle was connected to a high pressure extension line attached to a 6 ml Luer lock syringe via a three-way tap. The extension line was secured to the limb using a bandage (Vetrap®) taking care not to alter the position of the needle. The limb was then positioned within the MRI machine's (0.31T, O-Scan equine®, Esaote Veterinary) 200 mm coil to mimic the positioning of a horse in lateral recumbency.

Resistance to injection was carefully assessed; if resistance was encountered correct positioning of the needle was verified by removing the limb from the MRI machine and acquiring a lateromedial radiograph. The limb was subsequently replaced in the MRI machine, injection (5000 mm^3) completed and the images acquired.

2.4.2 MRI acquisition

MR images were acquired before and after injection of 5000 mm^3 of gadolinium contrast medium (2 mmol/L, Gadovist®) 2 mmol/L into the navicular bursa (NB). A coil with a field of vie of 200 mm was used. The isocentre of the coil was positioned at the level of the navicular bone on sagittal images. Post-injection images were T1 sagittal sequence for the experiment to identify anatomical landmarks for the bursa's boundaries; STIR, T2 FSE and TME PD-T2 sagittal sequences were used for the experiment measuring NB volume (appendix). Post-injection T1 frontal images were also acquired. Gadolinium was chosen for the description of the NB boundaries due to the improved contrast provided. For the volume measurement water was considered more appropriate due to similar intensity to synovial fluid in clinical cases.

Poor quality images were rejected and reacquired if due to technical problems; limbs consistently producing poor quality images were excluded from the study.

2.4.3 MRI anatomical landmarks of the navicular bursa

To visualise landmarks for the boundaries of the navicular bursa clearly, 5000 mm^3 gadolinium contrast medium (2 mmol/L, Gadovist®) 2 mmol/L were injected into the bursa of one forelimb prior to MRI (Nelson et al 2017). Injection and imaging were performed as described in sections 2.4.1-2.

Extensive use of the interactive, three-dimensional, anatomical guide (The Glass Horse Elements of the Distal Limb 2010 (https://www.sciencein3d.com/about.html)) was made to interpret the images.

2.4.4 3D Slicer®

Image quality was assessed subjectively by the observer prior to importing to the 3D Slicer® platform (https://www.slicer.org). Images of suitable quality were imported as DICOM files by clicking on the 'DCM' icon on the top left of the screen (Figure 2.0).

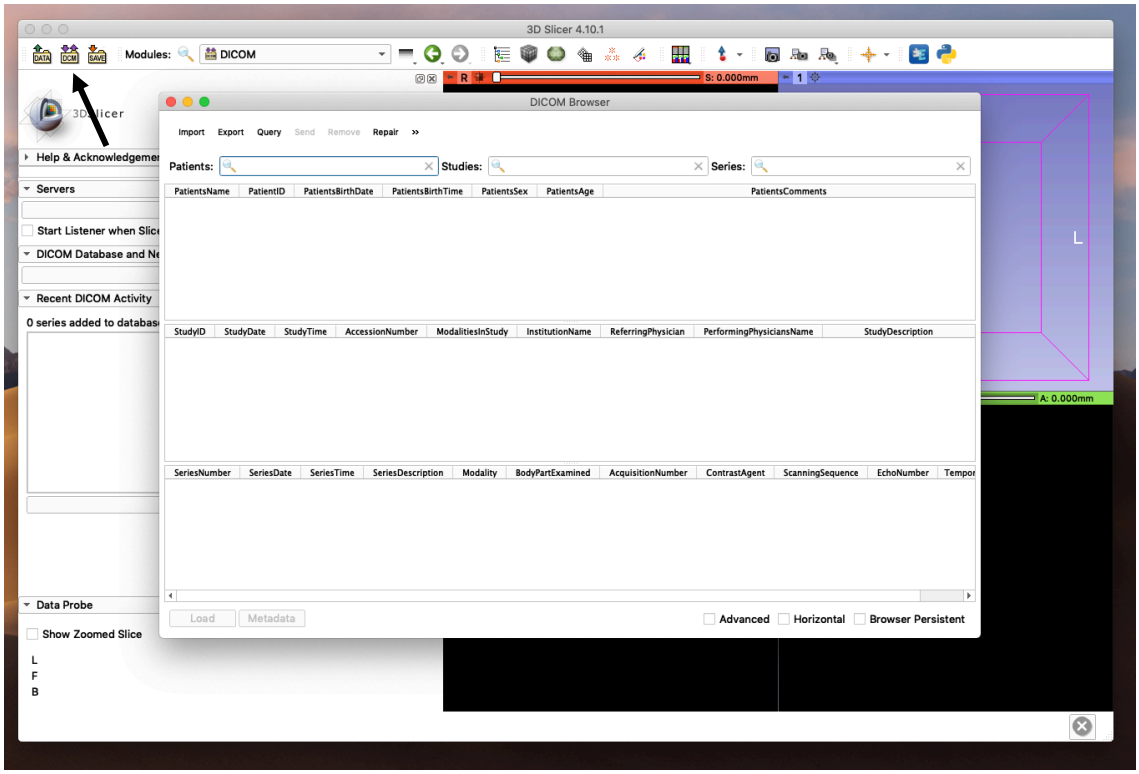

Figure 2.1. Screen shot showing the procedure to import DICOM files in 3D Slicer®. The 3D Slicer® software was opened and the 'DCM' (black arrow) icon on the top left of the screen selected. A window subsequently opened to allow the observer to retrieve the DICOM file from a folder on the computer.

In order to perform the measurements using 3D Slicer®, the window 'yellow slice only' was selected and the image magnified to visualise better the region of interest (the NB). The 'editor' option was then selected from the top bar menu (Figure 2.1).

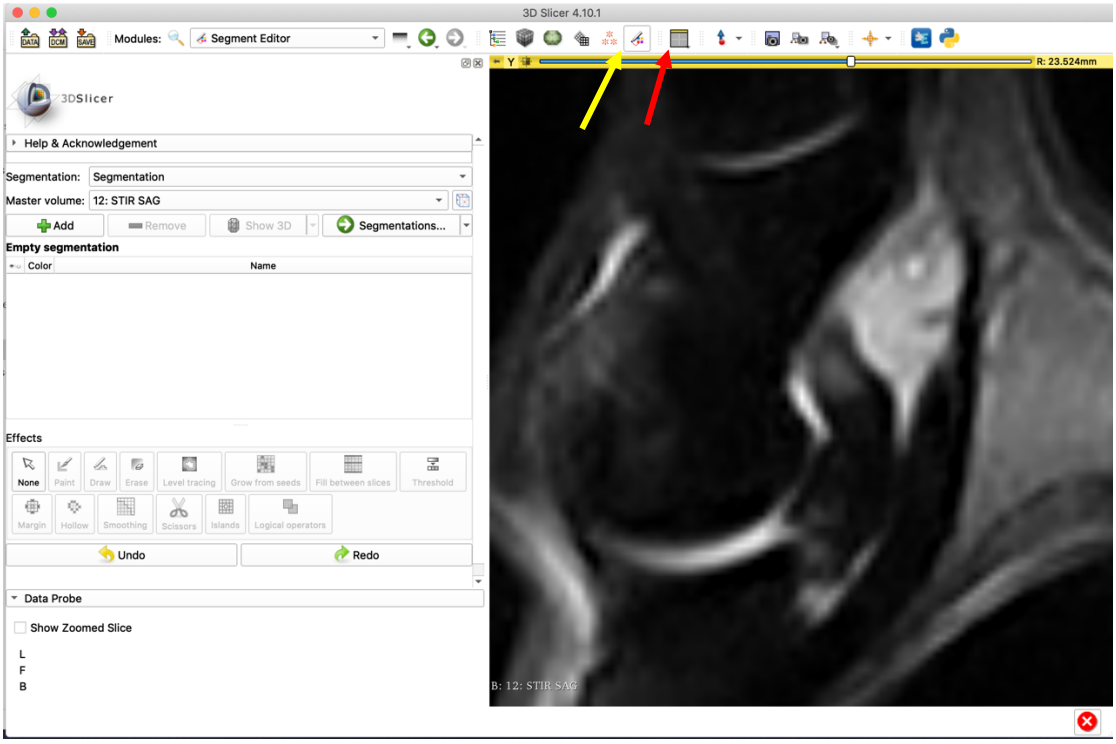

Figure 2.2. Screen shot showing the selection of the 'yellow slice only' option and 'editor' menu in 3D Slicer®. From the top bar the 'yellow slice only' option was selected (red arrow). This allowed magnification of the NB in order to visualise better the NB boundaries. The editor menu was then selected (yellow arrow).

The 'paint effect' tool was selected to highlight fluid within the NB in the MR images (Figure 2.2). 'Fluid' (light blue colour) was chosen as a colour option from the generic colour atlas menu. This required identification of the NB's boundaries and the fluid contained within them. The signal associated with the proper palmar digital artery within the solar canal was used as a reference for the signal intensity of fluid because of its convenient anatomical location adjacent to the bursa and it is consistently fluid-filled (liquid – blood clot in cadaver specimens) (Figure 2.3). The area corresponding to the NB was therefore selected using 'paint tool' on each of the 19 saggital images available for both STIR and T2 FSE sequences. Fluids with high water content, such as blood and synovial fluid, produce high intensity signal in T2 FSE and STIR MRI sequences.

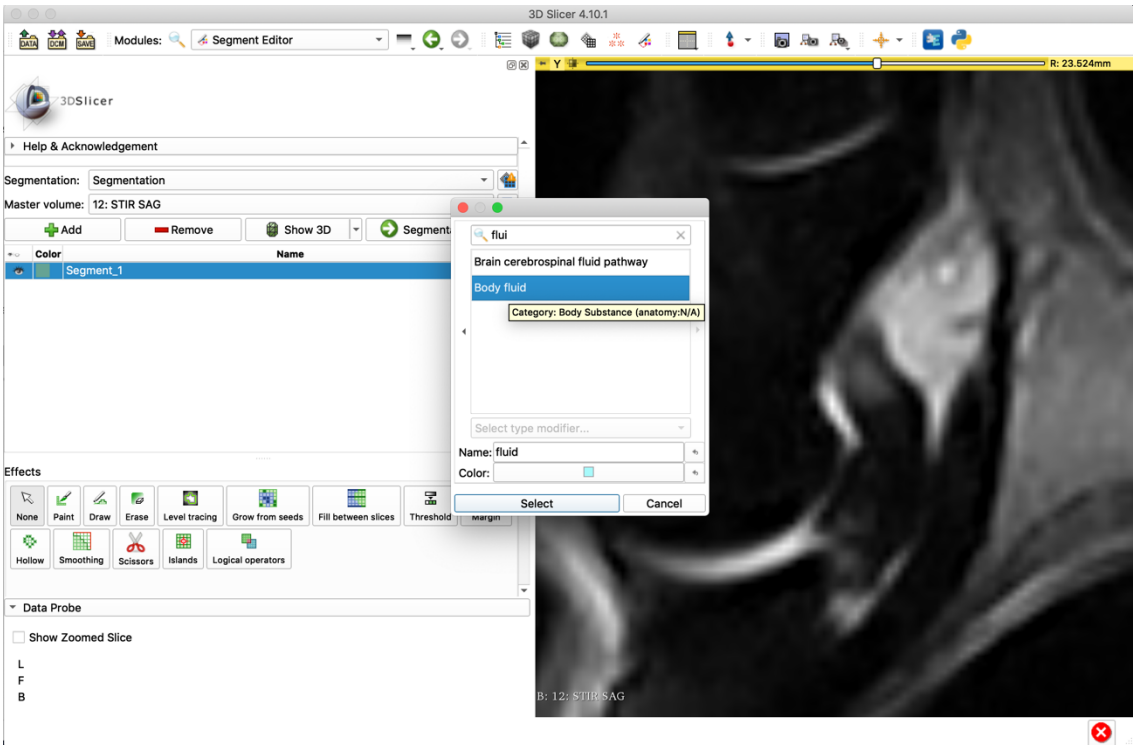

Figure 2.3. Screen shot showing the procedure to select the paint effect in 3D Slicer®. After selection of the 'paint effect', the blue colour was selected from the colour menu.

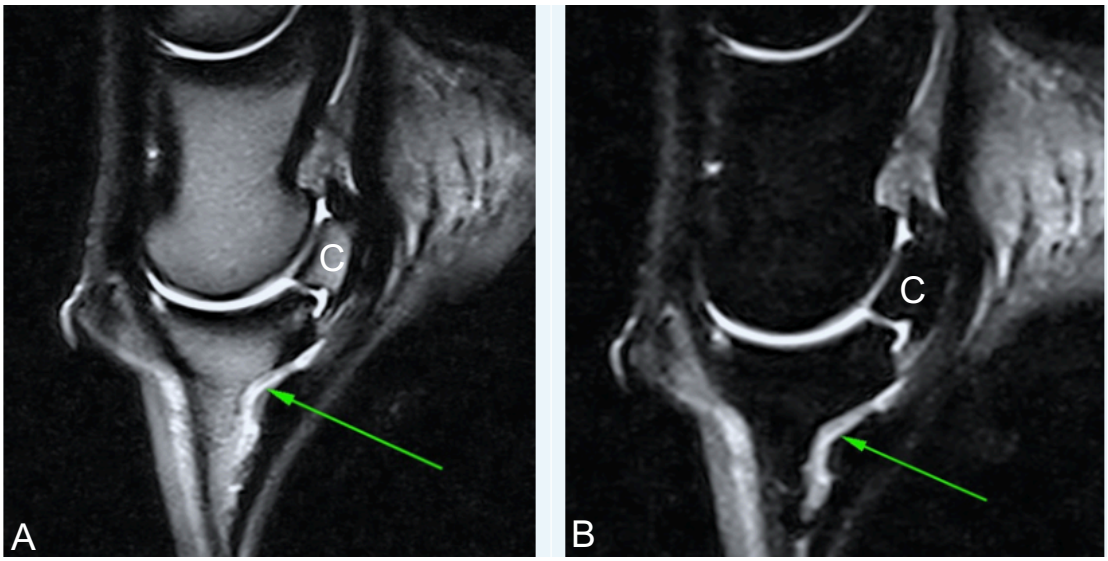

Figure 2.4. Image showing the intensity reference for use during navicular bursa (NB) volume measurement. Sagittal T2 (A) and the STIR (B) images are shown. The intensity corresponding to the proper palmar digital artery is indicated by the green arrow. C is the navicular bone.

Once the NB was highlighted on all slices, the option ‘make a model’ was selected and the volume of the model was automatically calculated in mm^3 (Figure 2.4).

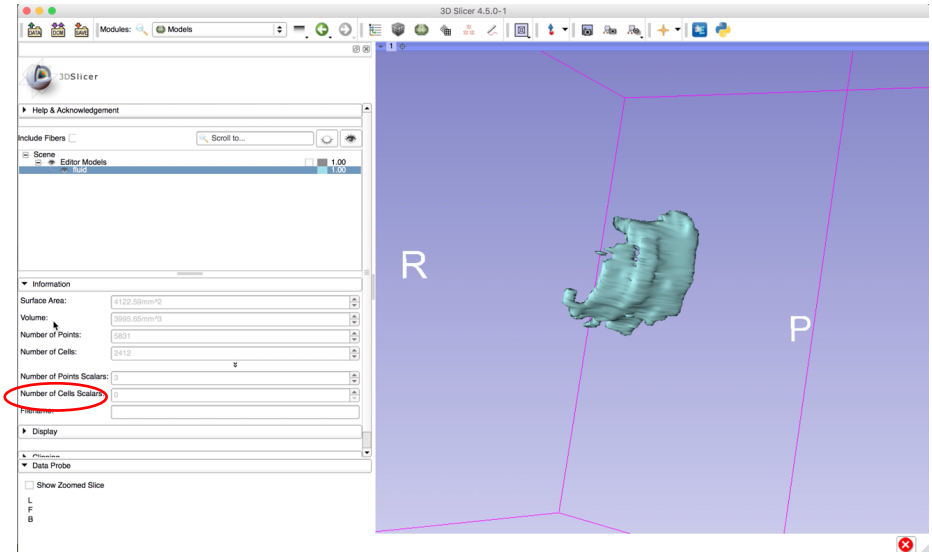

Figure 2.5. Screen shot showing the reconstructed volume of the NB using 3D Slicer®. After selection of the NB area using the paint tool, the three-dimensional reconstruction of the NB volume was performed and the volume measured displayed (red ring) in the information window.

Three separate reconstructions were performed for each volume of fluid injected.

2.4.5 Navicular bursa volume measurement – pilot experiment

In a pilot experiment, the navicular bursa of one forelimb was injected with 1000 mm^3 water initially and then a further 2000 mm^3 in 1000 mm^3 increments. Bursa volume measurements were made after each injection.

2.4.6 Data Analysis

All measurements were recorded in an Excel® (Microsoft®) spreadsheet in preparation for analysis. The mean of the three measurements was calculated for each volume of fluid injected.

2.5 Results

2.5.1 Cadaver specimens

Investigation	Number of distal forelimbs	Age, sex	Limb
Anatomical landmarks	One	2 yo gelding	Left
Volume measurement	One	2 yo gelding	Left

Table 2.1. Details of the cadaver specimens used in the work described in this chapter. All limbs were harvested from adult Thoroughbred horses.

2.5.2 MRI anatomical landmarks of the navicular bursa

The gadolinium within navicular bursa was visualised as very high intensity signal within the navicular bursa (NB) in the T1 MR images (Figure 2.5 B).

Figure 2.6. Sagittal MRI images obtained after gadolinium injection in the navicular bursa (NB). Note the increased signal intensity within the NB on the post-contrast image, improving visualisation of the NB boundaries. The dorsal boundaries of the NB are more easily identified (arrow). The navicular bone is labelled 'C'.

The gadolinium contrast studies of the navicular bursa (NB) facilitated identification of the following anatomical structures as landmarks of the bursa's proximal, distal and dorsoproximal boundaries, where the boundaries are not easily distinguished:

- *Proper palmar digital artery and terminal arch within the solar canal (continuation of the lateral and medial palmar digital arteries) (Figure 2.6)*: this was selected in order to avoid overestimation of NB volume by inclusion of the artery, which is located distally. This landmark can be identified on the mid sagittal plane and followed abaxially in medial and lateral directions.

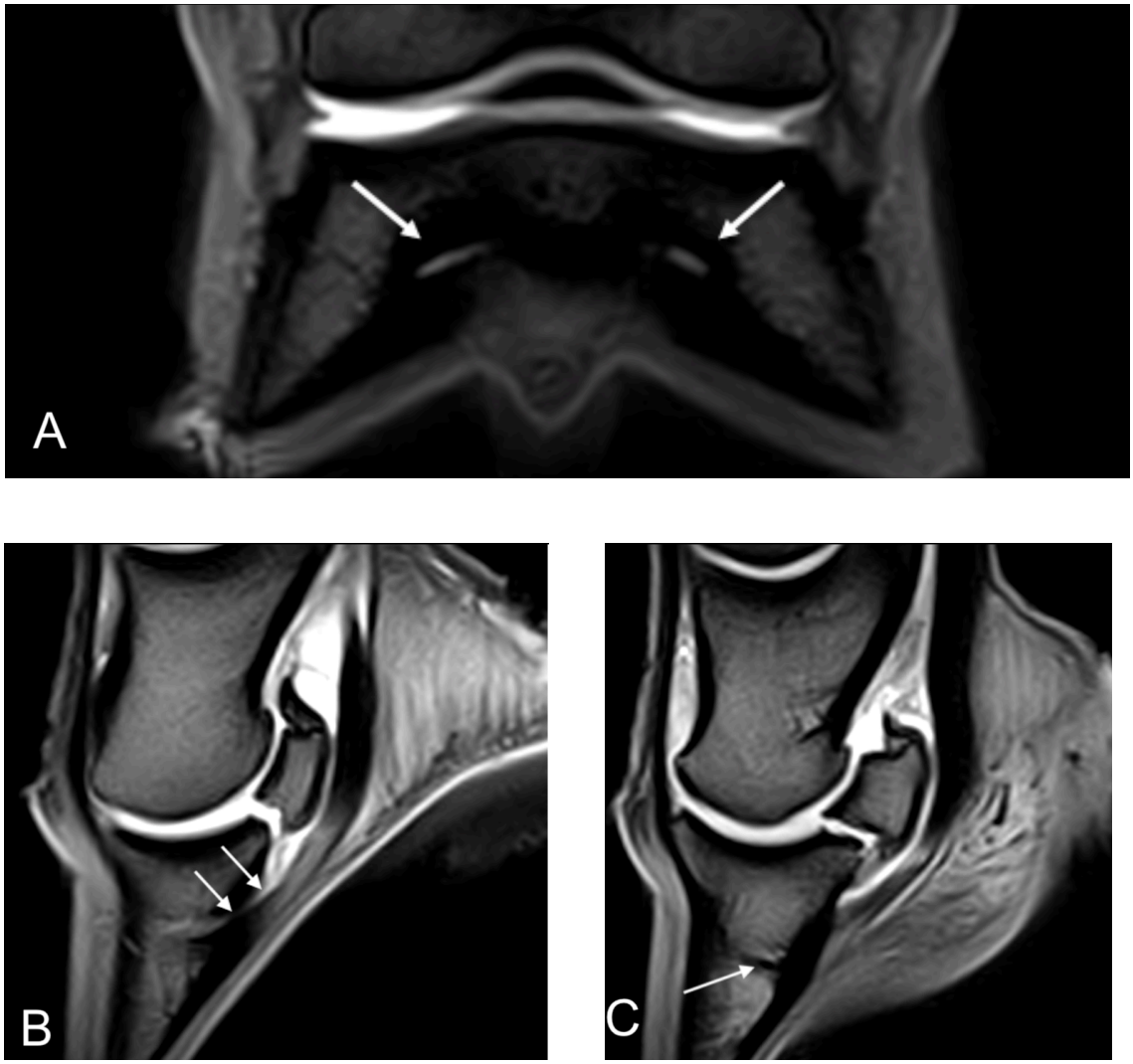

Figure 2.7. T1 MRI images acquired after gadolinium injection.Images acquired in frontal (A) and sagittal (B and C). In image A the arrows indicate the proper palmar digital arteries entering the third phalanx. Image B shows the solar canal of the proper palmar digital artery within the third phalanx (arrow). Image C shows a parasagittal section showing the path of the proper palmar digital artery (arrows).

- *Distal rami (artery and vein) of the navicular bone (Figure 2.7)*: this anatomical landmark was selected in order to improve recognition of the dorsodistal boundaries of the NB. They can be identified in the mid sagittal plane and followed abaxially in medial and lateral directions.

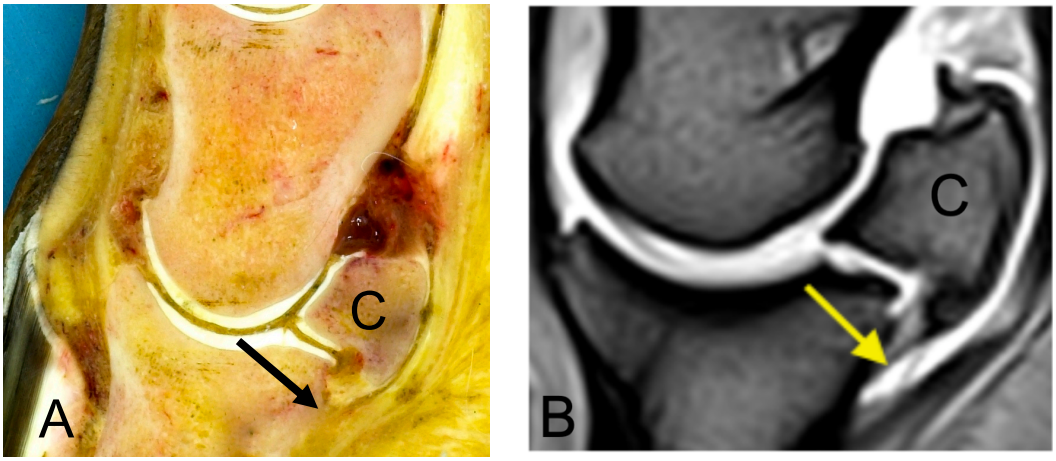

Figure 2.8. Image of anatomical specimen and MR image showing the distal rami of the navicular bone. The images are: (A) zoomed mid sagittal section of an equine digit centred on the navicular bone (C); and (B) a corresponding T1 MRI image acquired after gadolinium injection. The distal rami are identified by the arrow in both images.

- *Collateral sesamoidean ligament (Figure 2.8)*: these were identified in as landmarks to delineate the most dorsal extension of the proximal NB, and to avoid inclusion of a portion of the palmar aspect of the distal interphalangeal joint (DIPJ) when making measurements.

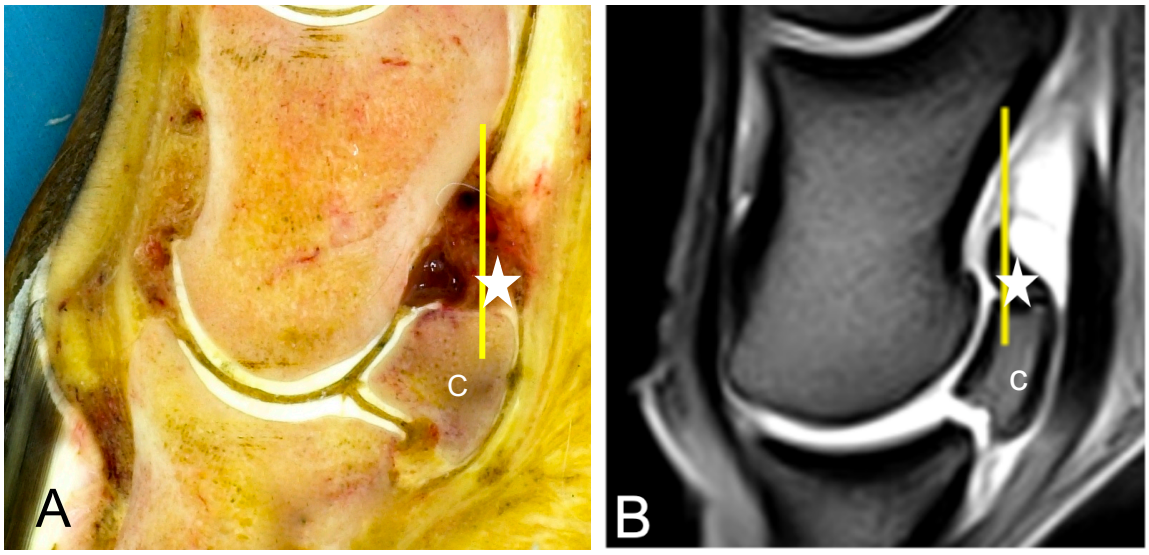

Figure 2.9. Images showing the dorsal limit of the navicular bursa (NB). The most dorsal extension of the NB is identified by the yellow line in a mid sagittal section from an anatomical specimen (A) and in a corresponding T1 MRI image acquired after gadolinium injection (B). The collateral sesamoidean ligament are identified by the star. C is the navicular bone.

- *Palmar rami of the (artery and vein) of the second phalanx (Figure 2.9)*: this landmark was used for the palmaroproximal extension of the NB.

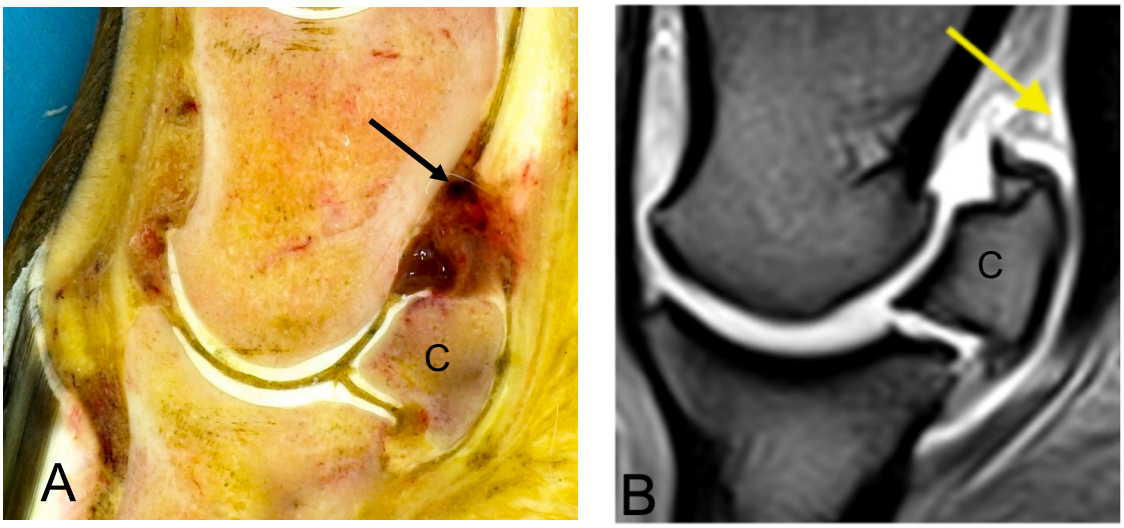

Figure 2.10. Anatomical image showing the palmar rami (artery and vein) of the second phalanx. The palmar rami are identified by the arrow in a mid sagittal section from an anatomical specimen (A) and in a corresponding T1 MRI image acquired after gadolinium injection (B). C is the navicular bone. Note: the proximal recess of the NB shows a minimal amount of effusion because most of the contrast medium has collected in the plantar abaxial pouches of the NB.

Figure 2.10 summarises the anatomical landmarks for the boundaries of the NB.

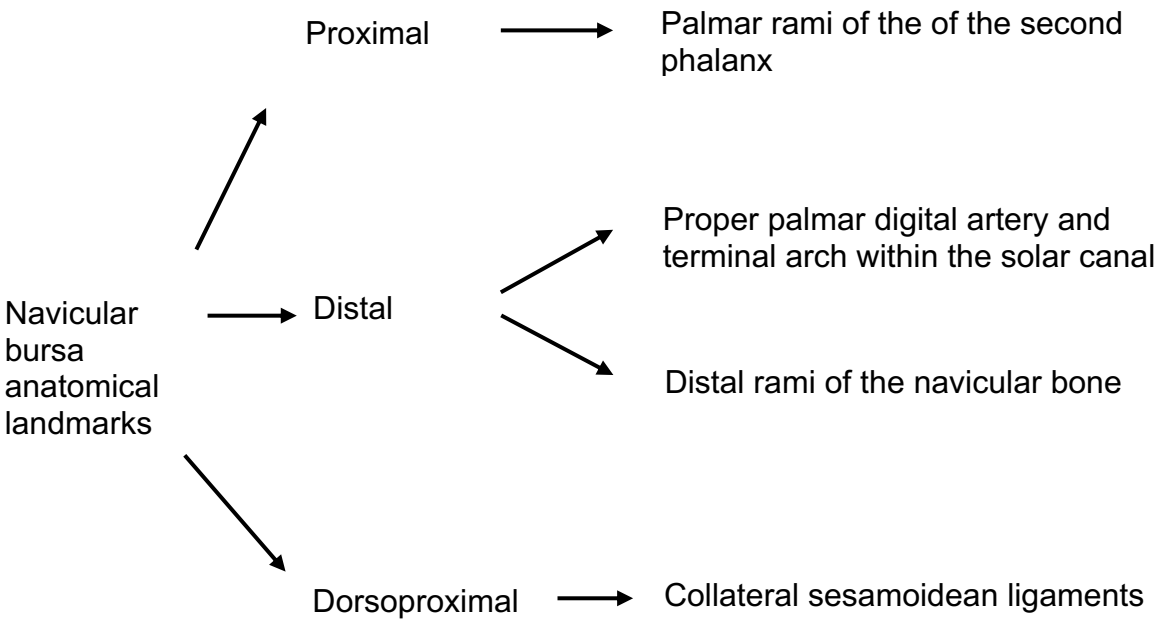

Figure 2.11 – Summary of the anatomical landmarks of the boundaries of the navicular bursa developed in this study.

2.5.3 Navicular bursa volume measurement using MRI and 3D Slicer®

The volume measurements made in the pilot experiment are shown in Table 2.1.

Volume of water injected mm^3	Volume measured – T2 FSE MRI sequence	Volume measured – STIR MRI sequence
1000	795.75	532.83
1000	699.83	486.17
1000	411.59	469.92
Mean (SD)	635.72 (199.94)	496.31 (32.66)

Table 2.2. Use of 3D Slicer® software to measure navicular bursa volume – measurements made from T2 FSE and STIR MRI sequences following the injection of 1000 mm^3 increments of water. The measured volume was the mean of three measurements). All measurements in mm^3.

The measurements made from both T2 FSE and STIR sequences were less than the volume of water injected into the bursa. For T2 sequence measurements, the underestimation was 36% on average when 1000 mm^3 were injected. The equivalent figure for STIR sequence measurements was 50%, indicating that underestimation was reduced when using T2 FSE rather than STIR sequences for measurements, even when accounting for the greater variability of the T2 FSE measurements (20% compared to 3% based on standard deviations).

2.6 Discussion

This *ex-vivo* study was performed in order to validate the use of a non-invasive, imaging based (MRI) method for the measurement of the navicular bursa (NB) volume using the 3D Slicer® computer program.

The results indicated that measurements from MR images underestimated NB volume but that the underestimation was reduced when using T2 FSE compared to STIR images. The volume measured from T2 images was consistently higher (reduced underestimation) than STIR (36% vs 50% of injected voluime respectively). In terms of performance, the opposite was true for the variability; the variability of STIR measurements was less than those from T2 FSE images (3% vs 20% respectively, based on standard deviations).

Sagittal images were chosen to perform NB volume measurements due to ease of interpretation of NB anatomy and superior orthogonal positioning (i.e. slices positioned perpendicular to the proximodistal extension of the NB) of the MRI slices compared to transverse images. Furthermore, the use of a sagittal sequence allowed visualization of the entirety (proximodistal extension) of the NB in a single image. This would not be possible using transverse images acquired using the conventional piloting of a routine MRI study of the equine foot because the examination requires separate proximal (including navicular bone and proximal aspect of NB) and distal transverse (including navicular bone and distal portion of NB) studies. For the method to be used on transverse images, development of an additional transverse study including the whole proximal to distal dimension of the NB would be necessary.

The difference in volume measurement between MRI sequences could relate to the poorer definition of STIR images (Bolas 2011). Also the reduced greyscale of STIR images and the sharper demarcation of fluid margins could have led to selection of a smaller area by the observer.

The influence of the volume averaging artefact should also be taken into consideration because it could have led to a smaller area being selected during the measurement process. However, the impact would be similar for both T2 FSE and STIR images. The artefact occurs when there is a mixture of different tissue types within a single voxel as this results in misleading pixel intensities in the image (Murray and Werpy 2011). This can hinder identification of structures with an edge or curved surface crossing multiple voxels or small structures (e.g. NB), which are either lost within one slice or partially cross, cut between or are separated into two slices because it leads to less well defined margins (e.g. of the NB boundaries). In order to minimise this artefact, the MRI slices were oriented perpendicular to the longitudinal axis of the NB (Murray and Werpy 2011). The volume averaging effect could have been minimised further by using a combination of sequences (allowing multiplanar visualisation) and including a higher resolution scan over the region of interest or by reducing the slice thickness (Murray and Werpy 2011). Although differently oriented sequences could have been acquired in this study to allow multiplanar visualisation of the NB,volume measurement from sequences oriented in different planes (e.g. sagittal and transverse) is currently not possible with 3D Slicer®.

Underestimation of the measured volume is likely to have been contributed to by leakage/diffusion of the water from the NB through the tissues and/or needle tract.

Observer error is another factor that could influence NB volume measurement because of its effect on selection of the area corresponding to fluid-filled bursa in each image. For this reason, clear anatomic landmarks for the boundaries of the NB and a reference for the signal intensity corresponding to bursal fluid were developed. The anatomical landmarks were identified using images acquired after injection of MRI contrast medium (gadolinium) to visualise clearly (due to marked hyperintensity of the contrast medium) the NB. The landmarks identified included the proper palmar digital artery and terminal arch within the solar canal, distal rami (artery and vein) of the navicular bone, collateral sesamoidean ligaments and

palmar rami (artery and vein) of the second phalanx. Additional benefits of the guidelines were perceived to be simplified training and quicker measurement.

The most realistic explanation for the underestimation of the NB volume identified in this chapter is a combination of leakage, observer error and volume averaging, rather than a single factor. The same factors can be considered responsible for an increased variability of the measurements performed on T2 FSE as opposed to STIR images. The reduced variability of STIR images is most likely related to the increased contrast of STIR images. It is possible that the increased contrast of STIR images reduces the variability of the area selected by the observer. In fact slice thickness and gap between slices is the same for both T2 FSE and STIR images.

In conclusion, the use of T2 FSE weighted MR images resulted in better estimation of NB volume compared to STIR images even when allowing for the increased variability of T2-based measurements. Therefore, the use of sagittal T2 FSE images was chosen to further investigate the performance of 3D Slicer® for the measurement of NB volume in the next chapter.

3 Validation of measurement of equine navicular bursa volume using low field MRI datasets and 3D Slicer® software

3.1 Introduction

The increased accessibility of advanced diagnostic imaging modalities (CT, MRI) in the last decades has led to increased interest in non invasive methods for assessment of synovial cavity volume (Heuck *et al* 1989, Ostergaard *et al* 1994, Ostergaard *et al* 1995, Ostergaard *et al* 1996). In more recent years the use of a fully automated system for the quantification of human joint effusion from MRI images was validated (Li *et al* 2010). In order to perform the study a 1.5T (high field) MRI machine was used in order to acquire T1 and T2-weighted sequences. The coefficient of variation following measurement of phantoms of different shapes (cylindrical and spherical) was found to be appropriate for use of the system in clinical cases (0.8-1.4%). Another group investigated the use of a semi-quantitative MRI method with or without contrast enhancement for the assessment of joint effusion and synovial membrane inflammation in human patients affected by knee OA (Loeuille 2011). This study concluded that contrast enhanced T1 sequences were superior for detection of synovitis. However, MRI scores for joint effusion obtained from T2 images were well correlated with joint volume measurement (synoviocentesis). The results obtained in this study (Chapter 2) support the use of T2 FSE images because the meaurements performed on T2FSE have increased accuracy compared to STIR images. Measurements obtained from T2w images resulted in underestimation of the navicular bursa (NB) volume by 36% compared to 50% when STIR images were used.

Based on the results obtained in Chapter 2 the accuracy and precision of NB volume measurements were made from T2 FSE sagittal MRI images. The intra- and inter-observer accuracy and precision were also calculated.

3.2 Aim

The aim of the experiments described in this chapter was to obtain data on the accuracy and precision of measurement of equine navicular bursa volume by post-

acquisition processing of T2 sequence MR images using 3D Slicer® (the method described in Chapter 2).

3.3 Objectives

The objectives for the experiments were to:

1. To investigate the correlation between the volume of water injected into the navicular bursa and the volume increase measured.

2. To assess the intra- and inter-observer agreement for measurements.

3.4 Hypothesis

The overall hypothesis for the project was: the accuracy and precision of measurement of NB volume from MR images in the horse using 3D Slicer® is sufficient for this method to be valuable in the investigation of lameness in clinical cases (i.e. ability to identify different degrees of NB effusion).

3.5 Materials and methods

The experiments performed in this chapter used the method developed in Chapter 2. Briefly, the navicular bursa (NB) of cadaver limbs was injected with water in 500 mm^3 increments until a total of 6000 mm^3 was injected. T2 FSE MR images were obtained before the first injection and then after every injection; NB volume was measured from the images using 3D Slicer®.

Four forelimbs were used for the experiment involving a single observer (the author), with NBs being injected with 6000 mm^3 in 500 mm^3 increments (i.e. there were four replicates of each volume injected). Imaging was performed once after each injection but measurements were repeated three times.

Three additional (blinded) observers performed volume measurements of NBs injected with 1000, 1500, 2000 and 2500 mm^3 in total. Three limbs were used for this particular experiment but the only replicate was the 2000 mm^3 volume; volume

measurements were made once. The observers recruited to the project were Diplomates in large animal surgery (two of the European College Veterinary Surgeons, one of the American College Veterinary Surgeons) who were familiar with the interpretation of MR images. They received 'hands on' training in the use of 3D Slicer® following an initial instructional session, were provided with reference materials showing the anatomical MRI landmarks of the NB (as described in Chapter 2) and were given the opportunity to practise measurements.

3.6 Data analysis

Volume injected and volume measured were recorded in a spreadsheet (Excel®, Microsoft UK) in preparation for analysis. Excel® was used to perform arithmetical calculations and statistical analyses, including plotting graphs, with the exception the Ryan-Joiner statistic for which Minitab® 19 was used (Minitab Ltd). The distribution of data was visualised as a frequency distribution histogram and tested for normality using Ryan-Joiner statistic as required.

For measurements made by the single observer, mean, standard deviation and median were calculated for navicular bursa volume, and for the increase in volume measured for each 500 mm^3 injection of water. The increase in volume for each 500 mm^3 injection was calculated from the cumulative volume measurements as follows:

Increase in volume = NB volume measurement after an injection of 500 mm^3 – NB volume measurement before

Box and whisker (volume measured against volume injected) and scatter plots (increase in volume measured for each injection against cumulative volume) were used to describe the data further.

Accuracy of the measurements was expressed as the difference between cumulative volume injected and volume measured, expressed as a percentage according to the formula:

Percentage accuracy = [NB volume (volume injected) – NB volume measurement]/NB volume x 100

Median was used as the summary statistic for accuracy; lower and upper quartiles of the percentage accuracy values were used to indicate precision of the measurements.

Similarly to the measurements made by a single observer, measurements made by multiple observers were recorded in Excel®. Mean and standard deviation were calculated, and accuracy and precision determined as described above.

3.7 Results

3.7.1 Cadaver specimens

Limb	Experiment		Age, sex	Left/right forelimb
	Single observer	Multiple observers		
1	✓	✓	2 yo gelding	Left
2	✓	✗	3 yo gelding	Right
3	✓	✓	3 yo gelding	Left
4	✓	✓	2 yo gelding	Right

Table 3.1. Details of the cadaver specimens used in the work described in this chapter. All limbs were harvested from adult Thoroughbred horses.

3.7.2 Single observer navicular bursa measurements

The single observer made three measurements of navicular bursa (NB) volume from the MR images following each injection in each limb (Tables 3.1 – 3.4), thus 12 measurements were made for each of the 12 injected volumes in the four limbs combined (a total of 144 measurements, Table 3.5).

The measurements, irrespective of volume or limb, were less than the injected volume except in four instances, indicating that the technique generally underestimated NB volume when used by this observer. The four exceptions were for volumes of 1500 mm^3 or less, three occurring when the total injected volume was 500 mm^3. This was consistent with an apparent trend for the underestimation

to increase with increasing volume injected, e.g. 7.9% for 500 mm^3 total volume compared to 63.3% for 6000 mm^3 total volume for Limb 1 based on the mean of the volume measurements (Table 3.1).

There were differences in the performance of the technique and/or observer between limbs with respect to underestimation (based on comparison of the means) and to the variability of the repeated measurements for any volume (based on comparison of the standard deviations). The latter also varied for measurements of the total volume injected for an individual limb without this variability being clearly related to increasing volume, suggesting that it was influenced by consistency in performance by the observer.

Trends in the measurements were explored further by summarising (Table 3.5) and representing the data graphically as a box and whisker pot (Figure 3.0). The graph confirmed underestimation of the total volume injected and visualised a change in magnitude once the volume reached 3000 mm^3 - underestimation was greater for injection volumes of 3000 mm^3, or above, than for volumes below 3000 mm^3. This was accompanied by an increase in the interquartile range, suggesting that there was also an increase in the variability of measurements made when injection volumes were 3000 mm^3 or above.

Transforming the data to examine the increase in volume measured for each successive 500 mm^3 injection of water into the NB (Figure 3.1 scatter plot of Table 3.6 data) clearly visualised the increase in underestimation of the measurements with increasing total volume injected. The change once a total of 3000 mm^3 had been injected was less clear than in the box and whisker plot of measurements of total volume however. This may be because the influence of leakage from the NB is reduced when considering the data in this way.

Plotting the increase in NB volume measurements (Table 3.6) as a frequency distribution histogram and calculation of the Ryan-Joyner statistic indicated that these data were not normal (results not shown). Accuracy and precision of the measurements were therefore described as median and lower/upper quartile respectively.

Median accuracy for the single observer was -40% for NB volume measurements made over the 500 – 6000 mm^3 range (the negative value indicated underestimation) (Table 3.7). Accuracy was better for volumes of 500 – 3000 mm^3 range (median -27%), which was consistent with the difference in the increased variability of measurements of 3000 mm^3 and above visualised in the box and whisker plot (Figure 3.0). The interquartile range for the accuracy statistics (used as an indication of measurement precision) was similar however for the two volume ranges: -54% to -26% (28%) for 500 – 6000 mm^3; -42% to -12% (30%) for the 500 – 3000 mm^3, presumably due to similarity in distribution of the data.

Volume injected mm^3	Mean volume measured	SD	Repeated volume measurements – Limb 1		
			1	2	2
0	~	~	~	~	~
500	460.33	126.69	603	361	417
1000	759.67	38.40	738	804	737
1500	1035.33	67.32	977	1109	1020
2000	1211.67	109.09	1086	1267	1282
2500	1407.67	60.37	1427	1340	1456
3000	1529.00	151.92	1362	1566	1659
3500	1566.67	91.47	1481	1556	1663
4000	1682.67	59.53	1642	1655	1751
4500	1745.67	140.59	1663	1666	1908
5000	1876.33	94.79	1917	1768	1944
5500	2017.33	80.64	1929	2036	2087
6000	2199.33	109.41	2073	2262	2263

Table 3.2. Use of 3D Slicer® software to measure NB volume - Limb 1 volume measurements. The NB was distended in 500 mm^3 increments from 0 until 6000 mm^3 had been injected in total. Three measurements were made for the cumulative volume after each injection (labelled as "1", "2" and "3"). Measurements made from T2 MRI sequence.

Volume injected mm^3	Mean volume measured	SD	Repeated volume measurements – Limb 2		
			1	2	2
0	~	~	~	~	~
500	515.67	63.96	461	500	586
1000	906.33	10.21	902	899	918
1500	1170.00	218.08	921	1327	1262
2000	1712.00	186.01	1899	1710	1527
2500	1696.33	190.42	1499	1879	1711
3000	1891.00	166.56	1700	2006	1967
3500	2096.00	245.30	1844	2334	2110
4000	2215.00	302.02	1897	2498	2250
4500	2233.33	298.34	1906	2490	2304
5000	2433.67	279.95	2115	2640	2546
5500	2503.33	243.52	2258	2745	2507
6000	2511.67	327.42	2159	2806	2570

Table 3.3. Use of 3D Slicer® software to measure NB volume - Limb 2 volume measurements. The NB was distended in 500 mm^3 increments from 0 until 6000 mm^3 had been injected in total. Three measurements were made for the cumulative volume after each injection (labelled as "1", "2" and "3"). Measurements made from T2 MRI sequence.

Volume injected mm^3	Mean volume measured	SD	Repeated volume measurements – Limb 3		
			1	2	2
0	~	~	~	~	~
500	405.67	32.01	405	374	438
1000	877.67	7.64	886	871	876
1500	1453.00	86.16	1370	1542	1447
2000	1954.00	100.86	1905	2070	1887
2500	2225.00	92.46	2119	2289	2267
3000	2593.67	70.32	2513	2642	2626
3500	2778.33	47.82	2724	2814	2797
4000	2980.67	12.74	2966	2987	2989
4500	3222.33	54.59	3166	3275	3226
5000	3415.00	79.32	3349	3503	3393
5500	3642.33	11.50	3654	3642	3631
6000	3675.33	38.42	3699	3696	3631

Table 3.4. Use of 3D Slicer® software to measure NB volume - Limb 3 volume measurements. The NB was distended in 500 mm^3 increments from 0 until 6000 mm^3 had been injected in total. Three measurements were made for the cumulative volume after each injection (labelled as "1", "2" and "3"). Measurements made from T2 MRI sequence.

Volume injected mm^3	Mean volume measured	SD	Repeated volume measurements – Limb 4		
			1	2	2
0	~	~	~	~	~
500	322.00	59.43	364	254	348
1000	639.33	126.06	496	733	689
1500	847.67	73.93	803	807	933
2000	1104.67	117.05	1006	1234	1074
2500	1395.67	84.68	1308	1477	1402
3000	1615.00	104.59	1508	1717	1620
3500	1844.67	140.76	1683	1911	1940
4000	1939.33	150.98	1765	2025	2028
4500	2035.33	223.57	1782	2205	2119
5000	2149.00	65.02	2085	2215	2147
5500	2252.33	214.40	2015	2432	2310
6000	2347.33	172.57	2150	2470	2422

Table 3.5. Use of 3D Slicer® software to measure NB volume - Limb 4 volume measurements. The NB was distended in 500 mm^3 increments from 0 until 6000 mm^3 had been injected in total. Three measurements were made for the cumulative volume after each injection (labelled as "1", "2" and "3"). Measurements made from T2 MRI sequence.

Volume injected mm^3	Mean volume measured	SD	Median	Repeated volume measurements											
				Limb 1			Limb 2			Limb 3			Limb 4		
				1	2	3	1	2	3	1	2	3	1	2	3
0	~	~	~	~	~	~	~	~	~	~	~	~	~	~	~
500	425.92	100.33	411.00	603	361	417	461	500	586	405	374	438	364	254	348
1000	795.75	124.02	837.50	738	804	737	902	899	918	886	871	876	496	733	689
1500	1126.50	254.70	1064.50	977	1109	1020	921	1327	1262	1370	1542	1447	803	807	933
2000	1495.58	382.81	1404.50	1086	1267	1282	1899	1710	1527	1905	2070	1887	1006	1234	1074
2500	1681.17	365.33	1488.00	1427	1340	1456	1499	1879	1711	2119	2289	2267	1308	1477	1402
3000	1815.00	305.65	1708.50	1362	1566	1659	1700	2006	1967	2119	2289	2267	1508	1717	1620
3500	2025.25	415.56	1925.50	1481	1556	1663	1844	2334	2110	2513	2642	2626	1683	1911	1940
4000	2204.42	528.37	2026.50	1642	1655	1751	1897	2498	2250	2966	2987	2989	1765	2025	2028
4500	2224.75	514.42	2026.50	1663	1666	1908	1906	2490	2304	2966	2987	2989	1765	2025	2028
5000	2468.50	621.23	2181.00	1917	1768	1944	2115	2640	2546	3349	3503	3393	2085	2215	2147
5500	2603.83	666.89	2371.00	1929	2036	2087	2258	2745	2507	3654	3642	3631	2015	2432	2310
6000	2683.42	631.23	2446.00	2073	2262	2263	2159	2806	2570	3699	3696	3631	2150	2470	2422

Table 3.6. Use of 3D Slicer® software to measure NB volume – volume measurements for the four limbs combined, shown as cumulative injected volume. Measurements made from T2 MRI sequence and are in mm^3. Data from Tables 3.2 - 3.5.

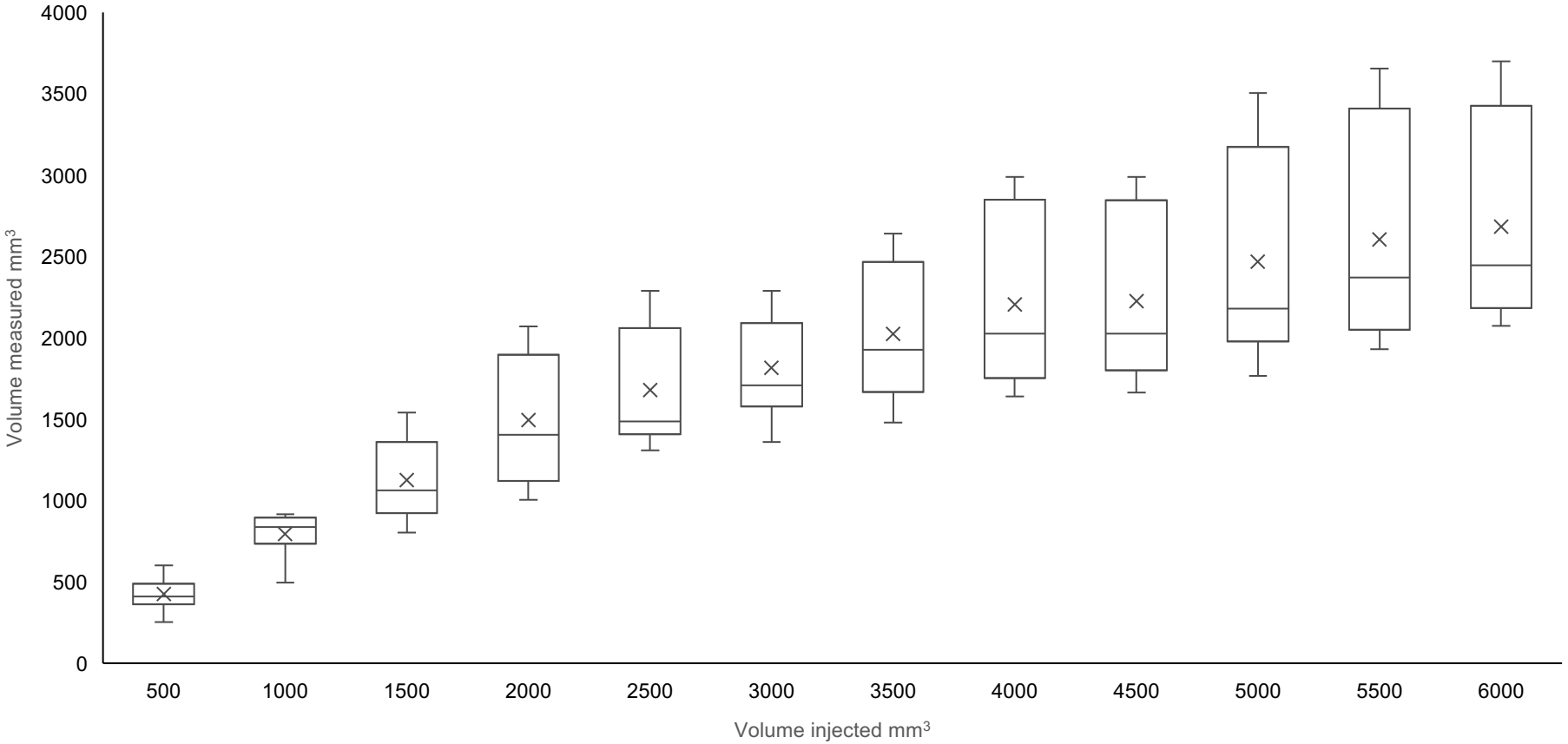

Figure 3.1. Use of 3D Slicer® software to measure NB volume – box and whisker plot of volume measurements for the four limbs combined against cumulative volume injected. Data from Table 3.5. Measurements made from T2 MRI sequence and are in mm^3.

Cumulative volume injected mm^3		Mean volume increase measured	SD	Repeated measurements *Negative values indicate a decrease*		
				1	2	3
Limb 1	0	~	~	~	~	~
	500	460.33	126.69	603	361	417
	1000	299.33	155.04	135	443	320
	1500	275.67	33.61	239	305	283
	2000	176.33	78.13	109	158	262
	2500	196.00	135.35	341	73	174
	3000	121.33	161.78	-65	226	203
	3500	37.67	70.78	119	-10	4
	4000	116.00	39.36	161	99	88
	4500	63.00	81.56	21	11	157
	5000	130.67	111.79	254	102	36
	5500	141.00	128.01	12	268	143
	6000	182.00	41.33	144	226	176
Limb 2	0	~	~	~	~	~
	500	515.67	63.96	461	500	586
	1000	390.67	54.98	441	399	332
	1500	263.67	216.01	19	428	344
	2000	542.00	382.17	978	383	265
	2500	-15.67	332.93	-400	169	184
	3000	194.67	64.73	201	127	256
	3500	205.00	106.52	144	328	143
	4000	119.00	58.40	53	164	140
	4500	18.33	32.04	9	-8	54
	5000	200.33	46.61	209	150	242
	5500	69.67	96.01	143	105	-39
	6000	8.33	92.96	-99	61	63
Limb 3	0	~	~	~	~	~
	500	405.67	32.01	405	374	438
	1000	472.00	30.51	481	497	438
	1500	575.33	93.58	484	671	571
	2000	501.00	52.94	535	528	440
	2500	271.00	94.43	214	219	380
	3000	368.67	22.14	394	353	359
	3500	184.67	22.81	211	172	171
	4000	202.33	35.64	242	173	192
	4500	241.67	44.19	200	288	237
	5000	192.67	31.63	183	228	167
	5500	227.33	83.51	305	139	238
	6000	33.00	28.93	45	54	0
Limb 4	0	~	~	~	~	~
	500	322.00	59.43	364	254	348
	1000	317.33	174.71	132	479	341
	1500	208.33	120.53	307	74	244
	2000	257.00	150.45	203	427	141
	2500	291.00	43.55	302	243	328
	3000	219.33	20.03	200	240	218
	3500	229.67	78.81	175	194	320
	4000	94.67	17.01	82	114	88
	4500	96.00	81.61	17	180	91
	5000	113.67	164.21	303	10	28
	5500	103.33	152.52	-70	217	163
	6000	95.00	50.69	135	38	112

Table 3.7. Use of 3D Slicer® software to measure NB volume – volume measurements for the four limbs as increment for successive 500 mm^3 injections. Measurements used T2 MRI sequence.

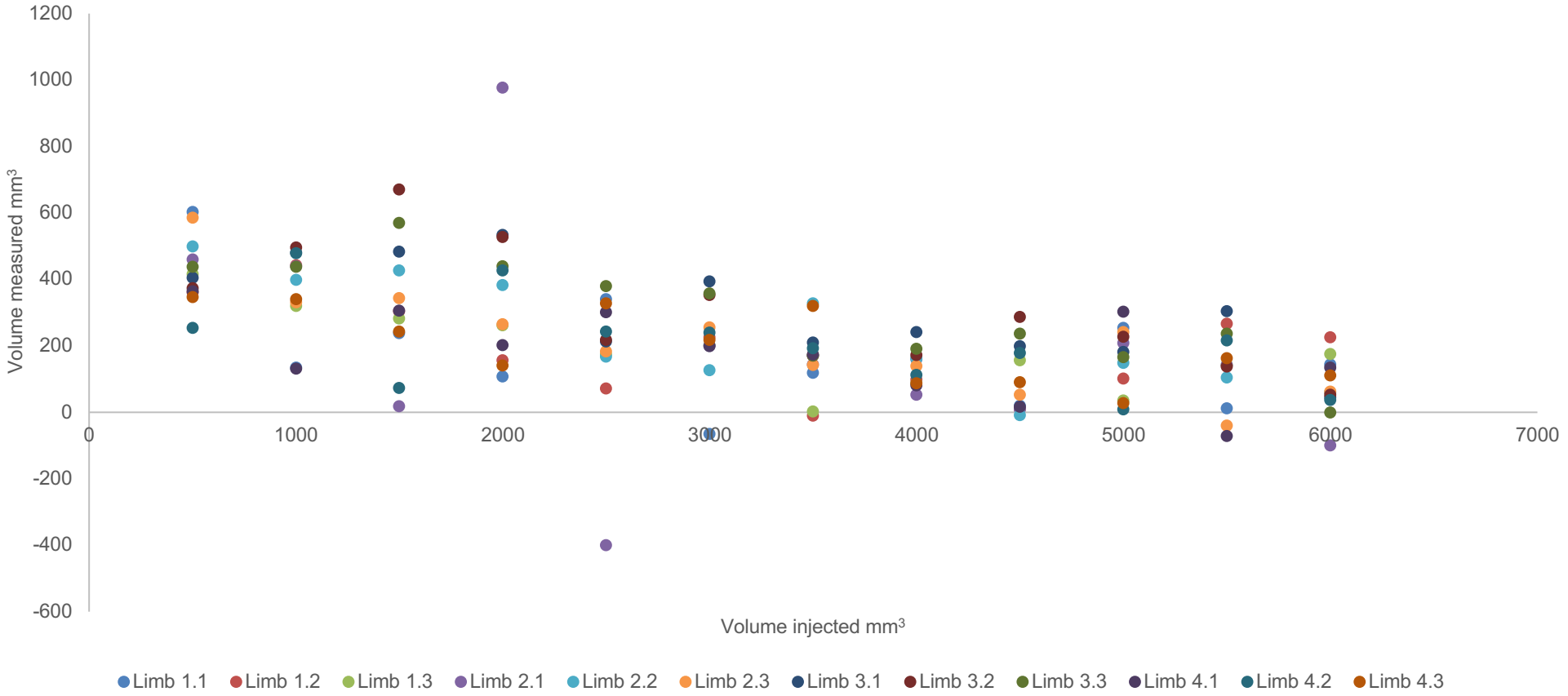

Figure 3.2. Use of 3D Slicer® software to measure NB volume – scatter plot of measurement of volume increases for the four limbs against cumulative volume injected. Data from Table 3.7. Measurements made from T2 MRI sequence and are in mm^3. "Limb 1.1", "Limb 1.2", "Limb 1.3" etc refer to the three measurements from each limb made after each injection. Negative values indicate a decrease in volume.

Formula: Volume injected – Volume measured, as percentage of volume injected

Volume injected mm^3	Limb 1 measurements			Limb 2 measurements			Limb 3 measurements			Limb 4 measurements		
	1	2	3	1	2	3	1	2	3	1	2	3
500	20.60	-27.80	-16.60	-7.80	0.00	17.20	-19.00	-25.20	-12.40	-27.20	-49.20	-30.40
1000	-26.20	-19.60	-26.30	-9.80	-10.10	-8.20	-11.40	-12.90	-12.40	-50.40	-26.70	-31.10
1500	-34.87	-26.07	-32.00	-38.60	-11.53	-15.87	-8.67	2.80	-3.53	-46.47	-46.20	-37.80
2000	-45.70	-36.65	-35.90	-5.05	-14.50	-23.65	-4.75	3.50	-5.65	-49.70	-38.30	-46.30
2500	-42.92	-46.40	-41.76	-40.04	-24.84	-31.56	-15.24	-8.44	-9.32	-47.68	-40.92	-43.92
3000	-54.60	-47.80	-44.70	-43.33	-33.13	-34.43	-29.37	-23.70	-24.43	-49.73	-42.77	-46.00
3500	-57.69	-55.54	-52.49	-47.31	-33.31	-39.71	-28.20	-24.51	-24.97	-51.91	-45.40	-44.57
4000	-58.95	-58.63	-56.23	-52.58	-37.55	-43.75	-25.85	-25.33	-25.28	-55.88	-49.38	-49.30
4500	-63.04	-62.98	-57.60	-57.64	-44.67	-48.80	-34.09	-33.62	-33.58	-60.78	-55.00	-54.93
5000	-61.66	-64.64	-61.12	-57.70	-47.20	-49.08	-33.02	-29.94	-32.14	-58.30	-55.70	-57.06
5500	-64.93	-62.98	-62.05	-58.95	-50.09	-54.42	-33.56	-33.78	-33.98	-63.36	-55.78	-58.00
6000	-65.45	-62.30	-62.28	-64.02	-53.23	-57.17	-38.35	-38.40	-39.48	-64.17	-58.83	-59.63

Summary statistics			
Volume range	Median	Lower quartile	Upper quartile
500-3000	-27%	-42%	-12%
500-6000	-40%	-54%	-26%

Table 3.8. Use of 3D Slicer® software to measure NB volume – comparison of the measurements made by a single observer to the volume injected (using data from Table 3.6). A negative value indicates underestimation.

3.7.1 Multiple observer navicular bursa measurements

Three observers (Observer A, B and C) made one measurement each of a navicular bursa injected with a total of 1000, 1500, 2000, 2000 and 2500 mm^3 of water (Table 3.8). In contrast to the measurements made by the single observer, the majority of measurements overestimated the volume injected (11 of 15 were overestimates, the remainder underestimates). The four measurements which underestimated the volume injected were made from the same limb (Limb 3), suggesting that the measurements were affected by factors associated with that limb. All four measurements made by Observer A overestimated the volume injected, and were greater than those made by Observer B and C.

The measures of accuracy and precision also indicated that the measurement technique performed differently when used by Observer A, B and C compared to the single observer, and differently when used by Observer A compared to Observer B and C (Table 3.9). Median accuracy for the three observers' measurements considered together was 54% but 32% for Observer B and C's measurements. The interquartile range for the accuracy statistics (used as an indication of measurement precision) was 5% to 78% (73%) and -17% to 52% (69%) for the two groups, respectively.

Limb	Volume injected mm^3	Mean volume measured	SD	Observer		
				A	B	C
1	2000	3297.67	1142.54	4614	2716	2563
3	1000	1107.00	541.41	1731	762	828
3	1500	1630.67	749.68	2495	1240	1157
4	2000	4182.00	1285.10	5644	3671	3231
4	2500	4715.33	1717.30	6693	3852	3601

Table 3.9. Use of 3D Slicer® software to measure NB volume – measurements made by three observers ("A", "B", "C"). Measurements made from T2 MRI sequence and are in mm^3.

		Formula: Volume injected – Volume measured, as percentage of volume injected		
Limb	Volume injected mm^3	Observer		
		A	B	C
1	2000	130.70	35.80	28.15
3	1000	73.10	-23.80	-17.20
3	1500	66.33	-17.33	-22.87
4	2000	182.20	83.55	61.55
4	2500	167.72	54.08	44.04

Summary statistics			
Observers	Median	Lower quartile	Upper quartile
A, B, C	54%	5%	78%
B, C	32%	-17%	52%

Table 3.10. Use of 3D Slicer® software to measure NB volume – comparison of the measurements made by multiple observers with the volume injected (using data from Table 3.8). A negative value indicates underestimation

3.8 Discussion

Underestimation of navicular bursa (NB) volume was a feature of the intra-observer part of the current study. The underestimation increased as the volume injected into the NB increased. For example, the underestimation calculated for the measurements performed on Limb 1 for a volume of 500 mm^3 vs 6000 mm^3 was 7.9% and 63.3% respectively.

The accuracy calculated for a volume equal or lower than 3000 mm^3 in the intra-observer part of the study was 27%. Similar accuracy (20%) was reported in a human medicine study in which the volume of the knee joint measured from MRI datasets was compared to the volume retrieved via synoviocentesis (Ostergaard *et al* 1995). The authors concluded that the accuracy of the method was acceptable in relation to the investigation of the use of effusion and synovial membrane volume as markers of the activity and/or severity of joint inflammation. This suggests that the accuracy of 27% for a volume of 3000 mm^3 or lower may be suitable for the use in equine clinical cases.

It has previously been reported that the NB volume is approximately 3000mm^3 based on the volume of contrast medium injected (Turner 1998). However, the volume of fluid present in the NB prior to injection was not taken into consideration in that report. Since the total volume of the NB corresponds to the sum of synovial fluid and volume injected it is not possible to rely on this statement when total volume of the NB is being investigated. Other authors reported that injection of a volume of 6000 mm^3 or greater can result in extravasation of fluid palmar to the deep digital flexor tendon (Maher *et al* 2011). Rupture of the NB was reported after injection of 10 000 mm^3 (Schramme *et al* 2009). The variation in the volume injected in the above mentioned studies suggests that the NB is an elastic structure which can therefore distend to accommodate a large, and probably biologically irrelevant, volume of fluid. To date in the published literature there are no reports describing a method for objective measurement of the NB volume. Therefore, assessment of volume is currently performed subjectively.

The NB volume underestimation identified in this chapter' work can be explained by a combination of leakage, observer error and volume averaging artefact.

The amount of underestimation increased with an increase in the volume injected. This could be attributed to the increased leakage due to increased pressure within the NB with larger volumes. It has been reported that injection of a volume of 6000 mm^3 can result in fluid extravasation (Maher *et al* 2011). For this reason leakage is likely to be the most important variable responsible for underestimation in this *ex-vivo* study. However, in clinical cases the lack of needle penetration of the NB and the constant, and probably lower, pressures within the NB mean that leakage is unlikely to be important in clinical cases.

The increased variability identified for volumes equal to or higher than 3000 mm^3 could be explained by difference in the area selected by the single observer during the repeated measurements. The higher NB volumes could have altered the relationship between the boundaries of the NB and surrounding structures (i.e. proper palmar digital and terminal arch within the solar canal, distal rami (artery and vein) of NB, collateral sesamoidean ligaments and palmar rami (artery and vein) of the second phalanx). This could have affected the area selected by the observer who in turn adopted a more 'conservative approach' during the selection of the NB area compared to lower volumes. This is the second most important

variable that could have accounted for the underestimation observed. Underestimation would be reduced by implementing premeasurement training. The landmarks identified in Chapter 2 represent useful guidelines that can be used for training purposes prior to NB measurement.

As mentioned in the development of the method phase of this Master's project (Chapter 2), volume averaging is another factor that could have contributed to the underestimation observed in the intra-observer part of the study. The effect of volume averaging could have been minimised further by using a combination of sequences (allowing multiplanar visualisation) and including a higher resolution scan over the region of interest or by reducing the slice thickness (Murray and Werpy 2011). However, this may not be applicable in a clinical setting due to the extra time needed. An MRI examination of both front feet with a standard protocol, as used in the current study, takes approximately 1 hour and 45 minutes. The acquisition of additional sequences would extend the duration of general anesthesia over 2 hours. This would significantly increase the risk of complication and mortality associated with general anesthesia (Tevik 1983; Young and Taylor 1990).

Only 4 out of 144 measurements obtained in the intra-observer part of the study represented an overestimation compared to the volume injected. Three of these measurements were obtained after the first injection (500mm^3) and one was obtained after the NB was injected with 1500 mm^3. The overestimation obtained in the intra-observer part of the study could be explained by the similar appearance (intensity) of closely related soft tissue structures. In fact if not completely separated by interposition of fluid synovial proliferation and/or hypertrophy of the DDFT, collateral sesamoidean ligaments, and/or DSIL have similar signal intensity (Maher *et al* 2011).

When the inter-observer measurements were investigated overestimation was a clear feature. Eleven out of 15 measurements overestimated, and the remaining 4 measurements underestimated, NB volume. The overall accuracy for the three observers was 54%. The actual volumes measured in this part of the study were equal or lower than 2500 mm^3. As previously mentioned the close relationship of synovium, DDFT, collateral sesamoidean ligaments and DSIL provide a similar signal intensity (Maher *et al* 2011) that would therefore result in selection of a

greater area by the observer. Considering the relatively low volumes measured by the different observers this factor could explain the overestimation recorded.

Another factor that could account for overestimation is use of different size and position of the region of interest by different operators leading to selection of a greater area. It has been reported that this alone could account for a difference in measurements of 20-30% (Cimmino *et al* 2003).

Although pre-measurement training was provided (about 20 volume measurements) in this part of the study the results of this chapter suggest that enhancing observer's training would be beneficial in reducing the variation between observers. Future work should include asking different observers to perform multiple measurements. This would provide better understanding of the intra observer variability.

In conclusion, the results of the intra-observer *ex-vivo* experiment showed that there is a significant relationship between the volumes injected and measured using 3D Slicer®. The overall accuracy and variability of the measurements performed by a single observer was superior to those of multiple observers. The NB volume underestimation was increased for volumes greter than 3000 mm^3. The accuracy of the intra-observer part of the study is considered adequate for the use of this method in clinical cases. Based on the results of the inter-observer study the use of this method for the measurement of the NB volume can be recommended in clical cases provided that training on anatomical landmerks and selection of uniform windowing are selected.

4 Use of 3D Slicer® platform as a planning and intraoperative aid in the management of a clinical case affected by deep digital flexor tendon (DDFT) core lesion.

4.1 Introduction

The experience gained using 3D Slicer® during the initial part of this Masters project was considered to be a valuable addition in the management of clinical cases undergoing MRI examination as a part of lameness investigation.

This report illustrates the use of 3D Slicer® in a clinical case using a novel treatment technique. This allowed pretreatment measurement of the volume of the navicular bursa (NB), measurement of the deep digital flexor tendon (DDFT) lesion volume and planning pathway of the needle to reach the lesion.

4.2 History

A 12-year old Warmblood gelding presented to the Weipers Centre Equine Hospital, University of Glasgow for investigation of a acute right forelimb (RF) lameness. Clinical examination of the RF identified dorsopalmar and mediolateral foot imbalance. The horse was grade 3 (AAEP 1999) RF lame and diagnostic local analgesia (palmar digital nerve block) localised the source of pain to the foot. The mediolateral and dorsopalmar foot imbalance was evident during the radiographic examinationof the foot. laddition to than during radiographic examination it was possible to visualise a small avulsion fracture fragment from the medial distal margin of the navicular bone.

Initial management comprised medication of the distal interphalangeal joint with 5 mg triamcinolone acetonide (Adcortyl™), farriery to improve foot conformation and a controlled exercise programme.

4.3 Further Investigation

Following an unsatisfactory response to initial management, MRI examination of the RF foot was performed. This was done with the horse positioned in lateral recumbency under general anaesthesia with the foot positioned within the 200 mm coil of an 0.31T MRI machine (0.31 T O-Scan equine®, Esaote Veterinary). The following image sequences were obtained: FSE T2 Sag, TME PD-T2 Prox Trans, TME PD-T2 Dist Trans, STIR Sag, STIR trans and Turbo 3D T1 Dor.

MR examination visualised a large core lesion (19.08 mm length and 6.4 mm maximum cross-sectional width) in the deep digital flexor tendon (DDFT) distal to the navicular bone. The lesion was identified as an hyperintense region in TM PD-T2, Turbo 3D T1 and STIR sequences (Figure 4.1).

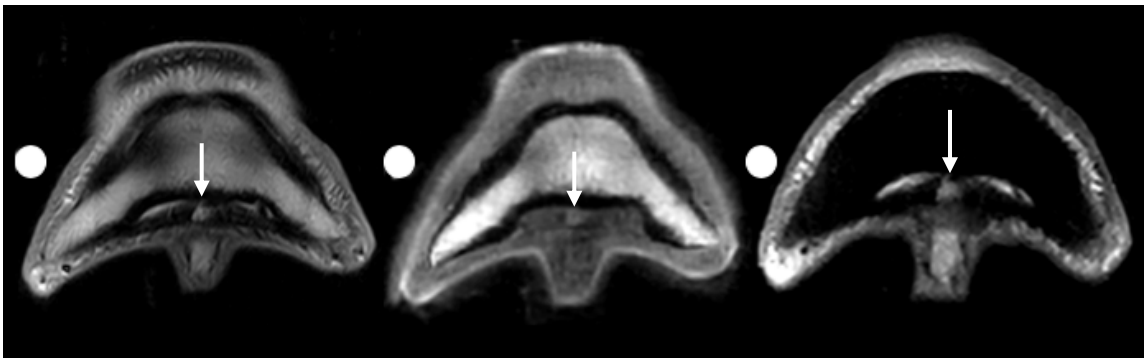

Figure 4.1. The figure shows the DDFT lesion as visualised on a distal transverse MRI sequence (Arrows). Note the hyperintensity of the lesion of T2 FSE (left), T1 (middle) and STIR (right) sequences. The white marked identifies the lateral aspect of the foot.

Due to the poor response of these lesions to conservative management (Dyson *et al* 2005) it was elected to treat the DDFT lesion by intralesional injection of platelet rich plasma (PRP) (Arnoczky and Sheibani-Rad 2013). The lesion location distal to the navicular bone within the foot precluded the use of ultrasonography to guide injection (Busoni and Denoix 2001); accurate needle placement would only be possible with MRI guidance.

4.4 Treatment

The horse's clinical presentation was unchaged when the horse returned to the hospital 8 weeks following the MRI diagnosis of a DDFT core lesion. Twenty-four hours prior to MRI guided injection the foot was aseptically prepared by paring and rasping the hoof capsule and the applying a bandage containing iodine solution (Vetasept®).

The previously acquired MRI images were uploaded onto the 3D Slicer® platform. Sagittal FSE T2-weighted REL images were used to measure the volume of the DDFT lesion and the volume of the navicular bursa (NB).

Sagittal FSE T2 REL, transverse TME PD-T2 and STIR images were acquired as previously described. The distance between the most proximal part of the DDFT lesion and the coronary band at the heel bulbs was 7.6 cm as measured using 3D Slicer® software.

After visualisation of the lesion using MRI the limb was removed from the coil and the area between the heel bulbs was aseptically prepared. In order to facilitate needle insertion (20 G 10 cm MRI Chiba Needle, Somatex®) a stab incision was performed using a N° 11 blade. A transcuneal ultrasonographic approach (Busoni and Denoix 2001) using a 12MHz linear probe (Vivid i, GE®, linear tendon probe 12L) was used to guide the initial needle direction by visualising the needle as far as the distal border of the navicular bone. Advancement of the needle was then monitored from the scale (expressed in cm) present on the needle shaft. When the correct depth was reached the needle and foot were protected by wrapping the foot and pastern in a sterile bandage (ethylene oxide sterilised Vetrap®) in preparation for repeat MR imaging (sagittal FSE T2 REL and transverse TME PD-T2 sequences). The needle was redirected twice before a satisfactory positioning was obtained.

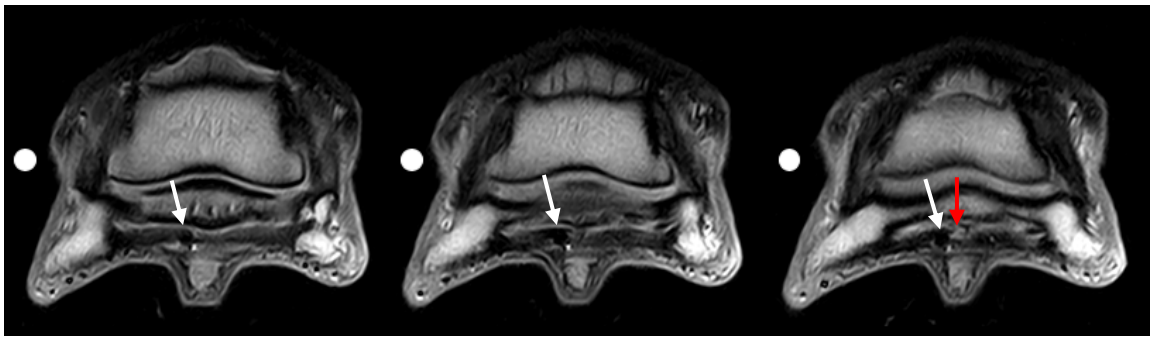

Figure 4.2. Transverse TME PD-T2 TRA magnetic resonance images in a palmar (left) to dorsal (right) sequence with needle in situ. Needle is visible as a circular signal void just lateral to the axial portion of the deep digital flexor tendon (white arrow); lesion is visualised as a focal hyperintensity (red arrow). The needle path is at the lateral border of the lesion but in the most dorsal image (right) the signal void and focal hyperintensity appear to coalesce.

Once correct positioning was confirmed (Figure 4.2), platelet rich plasma solution was injected using a luer lock syringe. The PRP was prepared during the anaesthetic period according to the manufacturer's instructions (V-Pet). Injection was performed until resistance was met – this was once 300 mm^3 had been injected. The foot was rewrapped in a sterile bandage for recovery from general anaesthesia.

Sequences used to perform volume measurement	**Date sequences were acquired**	**Volume measured mm^3**
TME PD-T2 TRA	24-11-2015	120
TME PD-T2 TRA	28-01-2016	210
	Difference volume measured mm^3	90
	Volume injected mm^3	300

Table 4.1. The table shows the measurement of the DDFT lesion. The sequence used and the date at which the MRI examination was performed are reported. Note the increase in lesion volume obtained prior to injection of the lesion.

The volume of the lesion measured from the images acquired at the time of diagnosis (2 months prior to the MRI guided injection was performed) was 120 mm^3. After the procedure was completed the volume of the DDFT core lesion was calculated for a second time from TME PD-T2 TRA images using 3D Slicer®. The measured volume was 210 mm^3. In the same occasion the volume of the NB was 478.61 mm^3 when measured using 3D Slicer® from TME PD-T2 SAG images.

Following the recovery from general anesthesia the horse received phenylbutazone (Equipalazone®) 2.2 mg/kg orally once daily. Box rest was prescribed for six weeks. During follow up assessment after 6 weeks' time the horse was sound on straight line and a moderate 3/5 RF lameness was noted on the soft surface during lunging on the right handside.

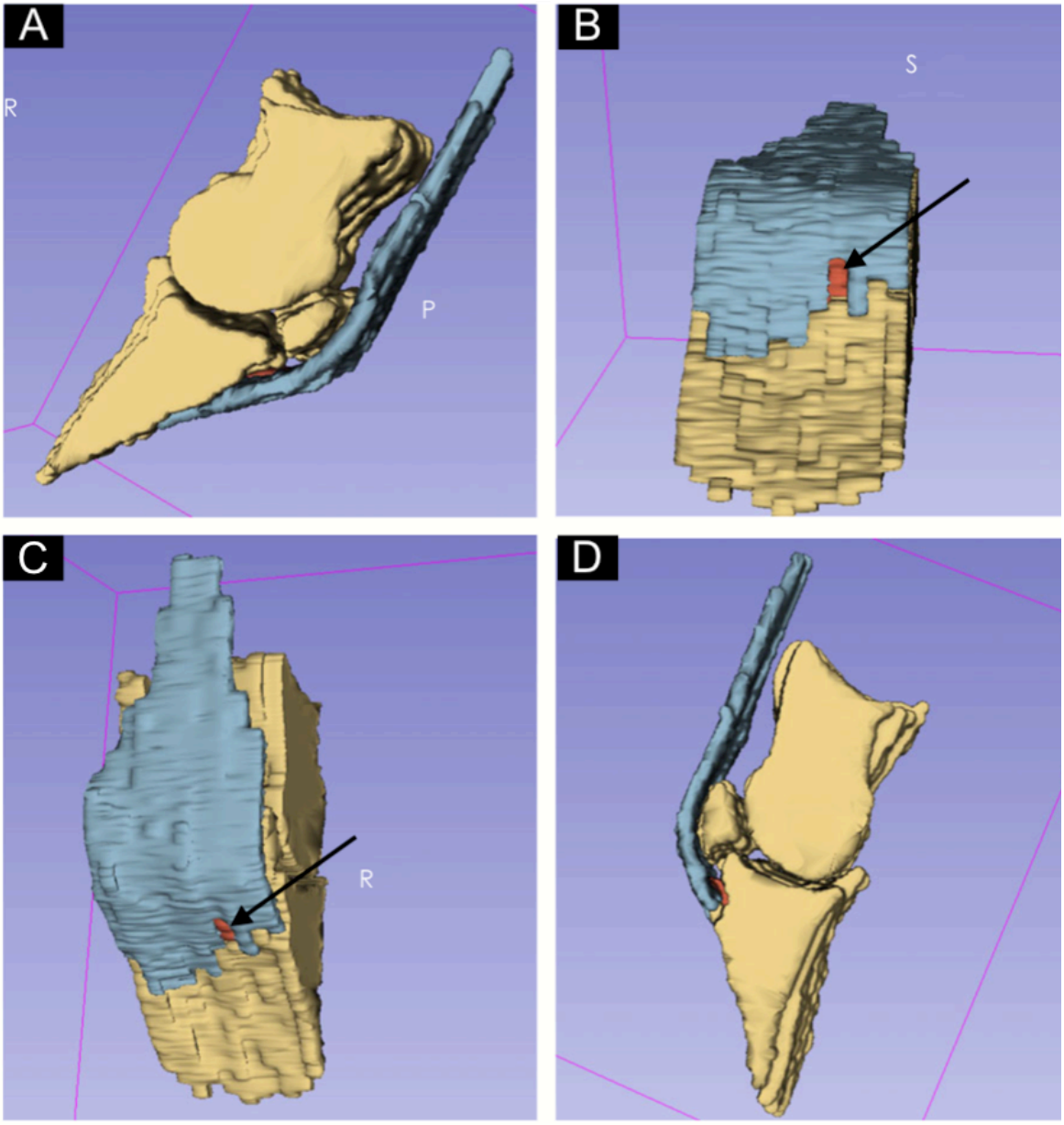

Figure 4.3 – Three dimensional reconstruction of the second phalanx, third phalanx, navicular bone (sand colour), DDFT (blue) and DDFT core lesion (red). The reconstruction was performed using 3D Slicer®. The Black arrow shows the DDFT lesion on the palmar views.

4.5 Discussion

The results of this study support the use of 3D Slicer® for planning and intraoperative guidance during MRI guided injection of DDFT core lesions.

The use of the free open source program 3D Slicer® for the measurement of volumes <1.13 cm^3 has been validated in a study in which subcutaneous tumour volume in mice was measured (Ma *et al* 2015). In this case report, application of 3D Slicer® allowed comparison of the volume of the DDFT core lesion before (at the time of diagnosis (24-11-15)) and after treatment (after MRI guided injection (28-01-16)). The volume measurement after intralesional injection of PRP resulted in an underestimation of the volume injected of about 30%. This discrepancy between the measured volume of the lesion and the volume injected was likely to have been the result of several factors. These are volume averaging artefact, observer error during selection of the area to be measured and selection of the correct intensity of signal when making measurements from MR images using 3D Slicer® (as described in detail relation to the work performed in Chapter 3) but also core lesion expansion as a result of increased pressure during PRP injection.

The poor structural differentiation of the injured tendon tissue resulting from haemorrhage, increased blood supply and oedema could have facilitated further expansion of the lesion during injection. Furthermore, tendon fibre degeneration has previously been recognised as a cause of DDFT lesions at the insertion onto the pedal bone (Busoni *et al* 2005) and therefore injection has the potential to disrupt weakened fibres.

The increase in lesion volume between the two time points at which measurements were made (67%) may be partly explained by progression of pathology. The potential for lesion volume to change over time means that measurement of lesion volume prior to injection is recommended. In addition to the risk of injecting too low a volume, there is a risk of injecting too high a volume which could cause further separation and disruption of tendon fibres. Measurement of DDFT lesion volume was performed in about 5 minutes.

This provides the clinician with valuable information if performed immediately before the injection. In cases where the treatment is carried out long after diagnosis (i.e. weeks) it is recommended to repeat the measurements in order to obtain an up to date measurement. Injection of a significantly larger volume could cause separation and further disrupt tendon fibres during the procedure due to the increased pressure.

The minimal amount of synovial effusion of the NB subjectively identified by the radiologist was confirmed by the low volume measured using 3D Slicer®. This can be explained by the fact that the DDFT lesion is located distal to the most distal aspect of the NB and therefore no direct communication between DDFT and NB is present. In fact when torn tendon or ligament fibers protrude into a synovial structure a marked inflammatory reaction with subsequent effusion of the same synovial structure is noted (Barker *et al* 2013).

T2 sequences were used to assess correct needle positioning to minimise needle artefact (Sequeiros *et al* 2005) and ensure good contrast between lesion and surrounding tendon. Other authors (Lamb *et al* 2014) have used T1 sequences to assess the correct needle positioning within the collateral ligament of the distal interphalangeal joint in horses. The increased tissue depth and small size of the target (DDFT) make the use of T2 sequences more suitable for this purpose.

Magnetic resonance imaging guided injection of DDFT core lesions within the foot is a novel concept that has never been reported before in the equine patient. A technique for MRI guided injection of DDFT lesions has recently been described in an ex-vivo study (Groom *et al* 2017). In the same study the limbs were positioned to reproduce the weight bearing position of horses under standing sedation. However, the use of standing MRI examination to guide DDFT injection has not been explored for the treatment of lesions located distal to the navicular bone such as the one described in this chapter. Due to the distal location and potential interference with the radiofrequency coil, it is recommended that the treatment of such lesions is performed with the patient under general anaesthesia.

The results of this case report support the use of 3D Slicer® for the assessment of volume of DDFT core lesions. The use of 3D Slicer® may be beneficial when performing MRI guided injection procedures.

5 Use of 3D Slicer® for the measurement of the navicular bursa volume in clinical cases

5.1 Introduction

The use of the 3D Slicer® platform for the measurement of the navicular bursa (NB) volume from MRI images proved to have the accuracy and precision that would potentially be appropriate for the measurement of NB volume in horses presented for MRI examination of the foot. The results of the *ex vivo* study (Chapter 3) showed that the use of sagittal T2-weighted MRI images for the measurement of NB volume resulted in a mean volume underestimation of 27% for volumes up to 3000 mm^3 and 40% for volumes between 3000 and 6000 mm^3. The method of NB volume measurement described in the *ex vivo* chapter was shown to be able to measure the increase in NB volume as well as total NB volume. We therefore hypothesised that the described method could potentially be used to establish the 'normal' NB volume and hence differentiate between 'normal' and 'abnormal' effusion. This would in turn allow establishing the volume of a normal NB, monitoring of NB effusion during repeated MRI examinations and also to assess the response to treatment. The measurement of the NB volume could therefore be used to support decision making during the management of clinical cases being investigated for lameness localised to the foot region.

In this study the volume of the NB measured using 3D Slicer® software in clinical cases was compared with subjective assessment by a boarded radiologist, which is currently considered the 'gold standard' for evaluation of NB effusion.

5.2 Aim

The aim of this study was to determine the feasibility of using an objective MRI based method for measuring navicular bursa volume in clinical MR images of the equine foot.

5.3 Objectives

The objectives of this study were as follows:

1. To determine the normal volume of the navicular bursa in horses without clinical signs of lameness.

2. To determine the volume of the navicular bursa in horses with clinical signs of lameness localised to the foot.

3. To determine whether the objective measurement method can differentiate between clinically normal horses and those with navicular region pathology.

5.4 Hypothesis

The hypothesis of this study is that an objective method can quantify the volume of the navicular bursa from clinical MR images and that the volume will be greater in horses with navicular region pathology.

5.5 Animals

Medical records of horses that underwent MRI between June 1st 2015 and January 31st 2018 at the Weipers Centre Equine Hospital, University of Glasgow and a database of equine MRIs maintained by a diagnostic imaging consultant were reviewed. All images were reviewed and interpreted by the same board-certified radiologist (Alexia McKnight DACVR).

Two groups of horses were included in the study; these were (1) a group of normal horses without signs of clinical lameness that underwent MRI as part of a pre-purchase examination and (2) horses with forelimb lameness localised to the foot by diagnostic analgesia.

The clinical data collected for each case were: foot examined (left forelimb (LF) or right forelimb (RF)), signalment, history (when available) and MRI diagnosis.

5.6 MR images

All horses included in this study underwent MRI using a low field MRI machine (0.31 T O-Scan equine®, Esaote Veterinary) under general anaesthesia.

TME PD-T2 weighted sequences acquired in the sagittal plane were included in the study. Image quality was determined to be satisfactory by the board certified radiologist prior to uploading the images onto the 3D Slicer® platform.

The board certified radiologist subjectively classified the cases based on their degree of navicular bursa effusion in 4 categories: normal, mild, moderate and severe effusion. All cases classified as normal underwent MRI examination as part of pre-purchase examination.

5.7 Image analysis

Navicular bursa volume measurement was performed by selecting the areas isointense with the signal of the proper palmar digital artery within the solar canal as described in the cadaver study (Chapter 2). The navicular bursa boundaries were identified using the previously described landmarks (Chapter 2). The measurements were performed a single time by a single observer (M Marcatili) on both T2-weighted sagittal images.

5.8 Statistical analysis

Statistical analysis was performed using one-way ANOVA for the effect of group (normal, mild, moderate or severe) on navicular bursa volume. To generate cut-off values to differentiate between normal/mild navicular bursa volume and moderate/severe navicular bursa volume, receiver operating characteristic (ROC) curves, a measure of the true positive response rate compared with the false positive rate, were generated. The area under the ROC curve was measured to assess the accuracy of these parameters to serve as a diagnostic test. Cut-off values were directly obtained from the ROC curves generated using commercially available graph and statistical software. Statistical analyses were performed using commercially available software (IBM SPSS®).

5.9 Results

All of the horses in the normal group underwent MRI as part of a pre-purchase examination. All horses in the mild and moderate groups were diagnosed with navicular syndrome. Four out of five horses with severe NB effusion had pathology

affecting the deep digital flexor tendon (DDFT) and one horse had navicular syndrome (Table 5.0).

Horse	Group	Limb	Signalment	Volume (mm^3)	Diagnosis
Case 1	Normal	LF	4 yo Quarterhorse Mare	1700.88	Pre-purchase examination
Case 2	Normal	LF	17 yo SSH mare	1208.03	Pre-purchase examination
Case 3	Normal	RF	N/A	1754.21	Pre-purchase examination
Case 4	Normal	LF	N/A	888.43	Pre-purchase examination
Case 5	Normal	RF	15 yo WB gelding	1059.19	Pre-purchase examination
Case 6	Mild	LF	18 yo TB gelding	799.41	Mild navicular bone stress injury
Case 7	Mild	LF	9 yo ISH	838.75	Mild navicular syndrome
Case 8	Mild	LF	13 yo TB gelding	1128.63	Moderate active navicular syndrome
Case 9	Mild	LF	6 yo WB gelding	1162.13	Mild navicular syndrome
Case 10	Mild	LF	10 yo ISH gelding	2004.90	Mild navicular syndrome
Case 11	Moderate	LF	N/A	1275.87	Moderate navicular syndrome
Case 12	Moderate	LF	8 yo WB gelding	3204.89	Erosive navicular bone disease
Case 13	Moderate	LF	10 yo ID mare	3568.79	Moderate navicular syndrome
Case 14	Moderate	RF	12 yo WB mare	1842.09	Moderate active navicular syndrome
Case 15	Moderate	LF	15 yo ISH gelding	3288.41	Navicular syndrome
Case 16	Severe	RF	3 yo WB gelding	5868.35	Mild navicular bone syndrome and dorsal border DDFT lesion
Case 17	Severe	RF	17 yo Appaloosa gelding	1781.24	Navicular bone and intrasubstance DDFT lesion
Case 18	Severe	RF	15 yo WB gelding	3783.32	Acute dorsal border DDFT tear
Case 19	Severe	LF	9 yo WB gelding	3002.81	Moderate active navicular syndrome
Case 20	Severe	LF	6 yo WB gelding	4726.97	DDFT septic disintegration

Table 5.1. Use of 3D Slicer® software to measure NB volume from MR studies – clinical cases. The degree of effusion as assessed by the board certified radiologist is shown in the first column. The limb undergoing MRI examination is shown in the second column. The diagnosis is stated in the final column. Volume measurements are in mm^3. DDFT= deep digital flexor tendon

The average of the measurements performed on T2 images with the corresponding standard deviation (SD) for the normal, mild, moderate and severe groups were 1322±387 mm^3, 1187±486 mm^3, 2636±1012 mm^3 and 3833±1569 mm^3 respectively.

The results showed that there was a statistically significant difference in the navicular bursa volume measured between bursae assessed as normal or as having mild effusion and severe effusion ($p<0.05$). There was no significant

difference when the comparison was between moderate and all the other groups (Figure 5.0).

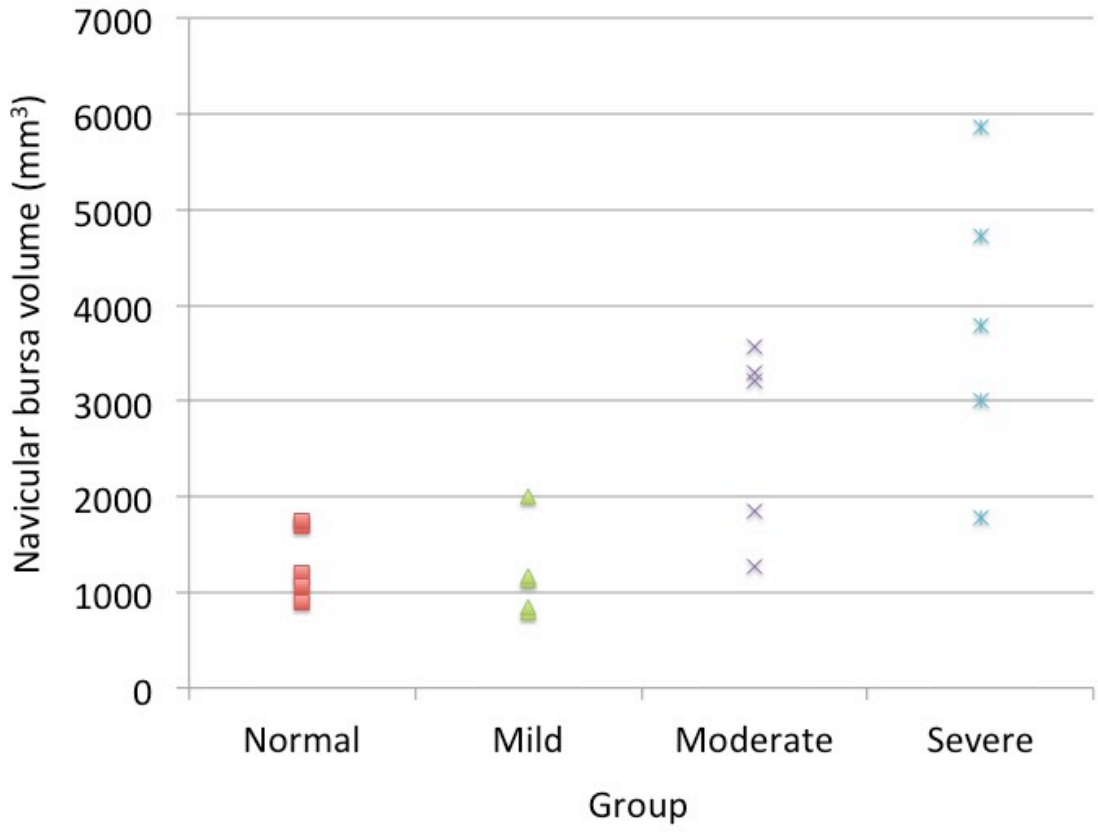

Figure 5.1: Dot plot displaying the navicular bursa volume measured on T2-weighted images for animals with either a normal navicular bursa or mild, moderate or severe navicular bursa effusion.

As there was no statistically significant difference between the normal and mild groups these data and the moderate and severe data were pooled for ROC analyses. Receiver operating characteristic analyses showed that the volume of the navicular bursa is a useful diagnostic test with an area under the curve of 0.95 (Figure 5.1). ROC analyses generated cut off values to distinguish between normal/mild navicular bursa volume and moderate/severe navicular bursa effusion. A volume of 1768 mm^3 was able to distinguish between normal/mild navicular bursa volume and moderate/severe navicular bursa effusion with 90% sensitivity and 90% specificity (Figure 5.2).

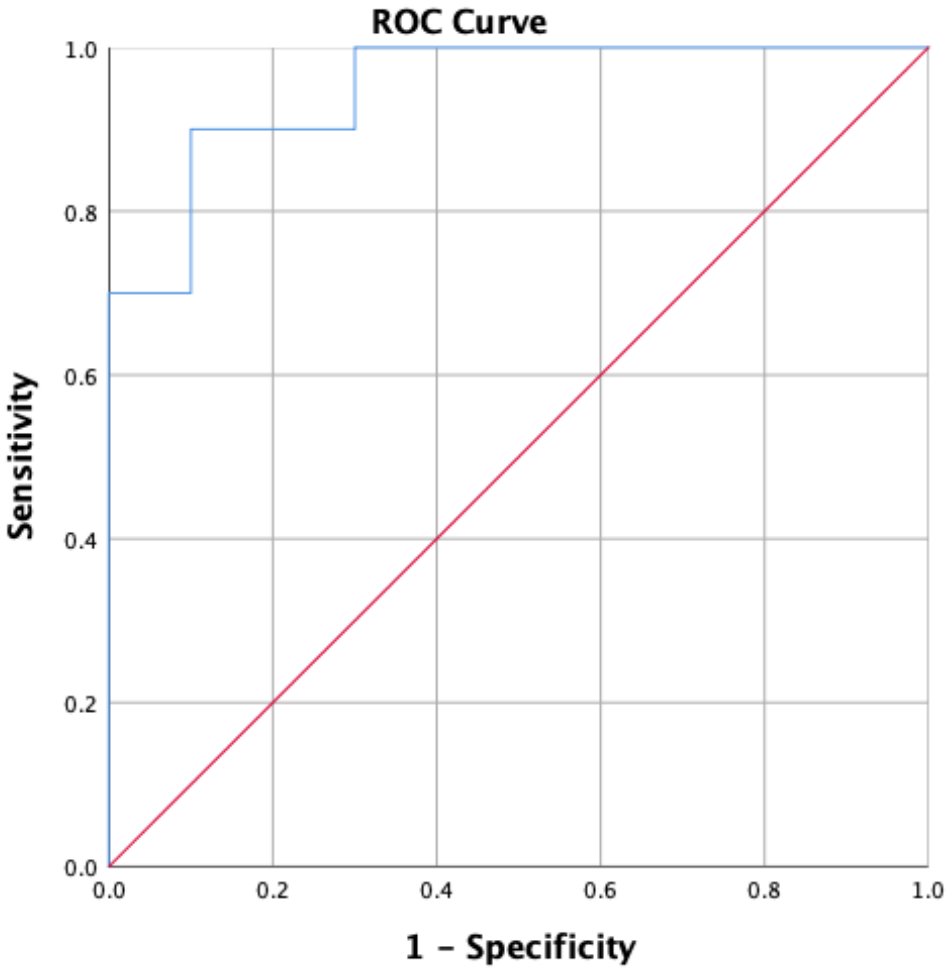

Figure 5.2: Receiver operating characteristic (ROC) curve for the volume of the navicular bursa. The area under the ROC curve was 0.95.

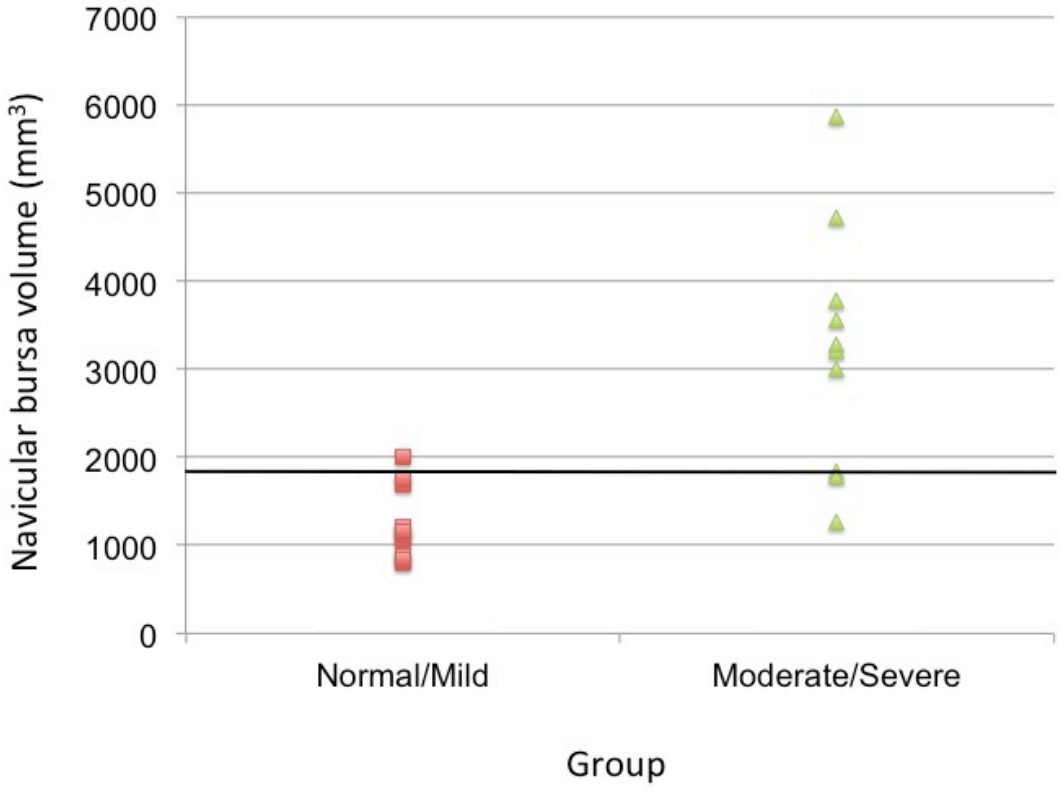

Figure 5.3: Dot histogram displaying the navicular bursa volume of horses with normal/mild navicular bursa volume or moderate/severe navicular bursa volume. The black line represents the cut-off value (1768mm^3) selected to distinguish between the normal/mild and moderate/severe groups.

5.10 Discussion

The results of this clinical study showed that subjective assessment (on a 4-point scale) of navicular bursa (NB) effusion (the current gold standard) resulted in poor differentiation of four different degrees of NB effusion. Differentiation between four different degrees of NB effusion on an ordinal scale was challenging for a person with considerable expertise in interpreting equine MR images. Clearer guidelines for subjective differentiation between normal, mild, moderate and severe NB effusion are therefore required in order to discriminate better between different degrees of effusion. However, the average difference of 135 mm^3 between normal and mild effusion may be difficult to appreciate even with improved guidelines. For this reason, the use of two instead of four degrees of NB effusion may be more appropriate (i.e. normal and effused). Therefore a decision was made to identify a cut off value that would allow differentiation between normal/mild and

moderate/severe effusion:a cut off of 1768 mm^3 is 90% sensitive and 90% specific to differentiate between normal/mild and moderate/severe.

The landmarks for the NB anatomy were well defined, making the area to be selected for measurement straightforward for the observer to select in the clinical cases. The degree of NB effusion did not have an appreciable effect, suggesting that the landmarks would be generally applicable to clinical settings.

Four out of five horses in the group with severe NB effusion were diagnosed with deep digital flexor tendon (DDFT) lesions based on MRI imaging. In three of these cases the lesions resulted in exposure of the tendon collagen tissue within the proximal recess of the NB. Fibers protrusion was identified by a signal void (hypointense signal on T2 ans STIR images) at the level of the proximal recess of the NB on transverse sequences. The presence of synovitis, leading to effusion, following collagenous tissue exposure has been reported for other synovial cavities such as the tarsocrural joint (Barker *et al* 2013). The identification of severe NB effusion in clinical cases should therefore prompt acquisition of additional sequences aimed at improving identification of DDFT lesions.

All the cases with mild or moderate NB effusion were diagnosed with navicular syndrome (objective NB volume measurement found no significant difference between these groups). The presence of NB effusion in horses with navicular syndrome could be explained by pathology of navicular bone fibrocartilage, even if this is not visualised with low field MRI without constrast bursography. Fibrocartilage degeneration is considered to be the earliest pathologic finding in navicular disease but cannot be clearly identified using low field MRI (Widmer *et al* 2000). Due to the poor visualisation of the NB fibrocartilage in low field MR images it is not possible to confirm whether there was a relationship between fibrocartilage damage and grade of NB effusion in the study population. Increased signal intensity in the spongiosa of the navicular bone in high field STIR images, which is a feature of navicular syndrome, can be associated with fibrocartilage lesions (Dyson *et al* 2012) and navicular bursography is 100% sensitive and specific for fibrocartilage lesions (Schramme *et al* 2009). Therefore, in order to define better the inciting cause of NB effusion in cases with navicular bone disease, high field MRI or magnetic resonance bursography should be considered.

In conclusion, the results of this study partially confirmed the hypothesis that subjective assessment of NB effusion in clinical cases discriminates successfully between different degrees of NB effusion. It was evident that subjective assessment of NB volume does not always correctly identify different degrees of NB effusion because subjective assessment was only able to discriminate between normal or mild effusion and severe effusion (when compared with an objective method of NB volume measurement).

Navicular bursa volume measurement using 3D Slicer® therefore potentially has a role in supporting subjective interpretation of MR images of the equine foot, particularly the assessment of NB effusion. If subjective assessment of NB effusion is used alone, the results of this study suggest that use of a scale with more than two degrees of effusion (normal and effused) is not reliable and could lead to error.

6 General discussion

The use of 3D Slicer® software as an objective method for the measurement of the navicular bursa (NB) volume in horses, which was validated as part of the work for this thesis, has proven to be a useful addition to clinical case management. Chapter 4 describes how 3D Slicer® was used to assist in the treatment of a deep digital flexor tendon (DDFT) lesion within the foot. In Chapter 5 3D Slicer® was used to assess the degree of NB effusion during MRI examination of the equine foot (Chapter 5).

Measurement of the volume of synovial structures is an area of growing interest in both human and veterinary medicine. Several methods have been investigated in both experimental and clinical trials in the last decades. These include those based on radioisotopic dilution (Rekonen *et al* 1973), albumin dilution (Geborek *et al* 1988), injection of high molecular weight dextrans (Delecrin *et al* 1992) and on calcium concentration (Matsuzaka *et al* 2002), although none is currently used in any clinical setting (human or veterinary). Joint volume measurement based on urea concentration in synovial fluid and serum has been described in equine practice (Kraus *et al* 2007). The use of an imaging method to measure synovial

structure volume in human medicine was first described in 1989 (Heuck *et al* 1989). The method took advantage of the development of MR and CT imaging, using three-dimensional processing of the images to determine volume. It was established that measurements were more accurate when MR images, rather than CT images, were used. The use of MRI as a tool for measurement of joint effusion in human clinical cases was assessed for the first time in 1994 (Ostergaard *et al* 1994). The authors used contrast (gadolinium) enhanced transverse T1-weighted images in calculating synovial fluid volume and found a high correlation between actual volume and measured volume. They therefore suggested that the method would be useful in the assessment of disease severity and response to treatment. The accuracy of synovial fluid volume measurement using this method was reported to be 20% (Ostergaard *et al* 1995). The use of contrast enhanced MRI was selected subsequently to assess the response to intra-articular medication with corticosteroids (Ostergaard *et al* 1996). The authors concluded that pre-treatment synovial volume may have predictive value for the response to treatment of rheumatoid arthritis in people (Ostergaard *et al* 1996). In 2010, a fully automated system for the quantification of human joint effusion from high field (1.5 T) MR images was validated using phantoms (Li *et al* 2010). The variation between measurements was small (0.8-1.4% coefficient variation), suggesting that the system could be used clinically. Unlike the *ex-vivo* part of our study (Chapter 2) in which distension of the navicular bursa in cadaver limbs was used to validate the method, two types of phantoms (two cylinders and a sphere) were used for validation. More recently semiquantitative MRI, with or without contrast enhancement (CE), has been used to evaluate synovial membrane inflammation and joint effusion in human patients affected by knee OA (Loeuille *et al* 2011). The results of this study showed a moderate correlation between MRI joint volume measurements and measurements based on arthrocentesis, although the exact volume of fluid was not calculated from MR images. T2w and T1w CE images performed similarly but the T1w CE images were more accurate for the assessment of synovial inflammation, especially cellular infiltration. The use of MRI to calculate the synovial tissue volume was explored further in 2016 (O'Neill *et al* 2016). The authors concluded that synovial fluid volume was better calculated from CE-MR images compared to pre-enhancement MRI images.

Although guidelines for NB volume (Turner 1998) and distensibility/capacity (Schramme *et al* 2009; Maher *et al* 2011) have been reported; to date in the

scientific literature no objective methods are described for the measurement of the navicular bursa volume.

The use of cadaver limbs was considered to be the best practical choice to validate the method for the measurement of navicular bursa volume from MRI datasets using 3D Slicer® (Chapter 2). After injection of gadolinium (2 mmol/L), the key anatomical landmarks were described in order to provide all the observers with clear guidelines. The preliminary data obtained from measurements on T2 and STIR MR images highlighted a greater accuracy of the measurements performed on T2 images as opposed to STIR measurements (36% vs 50% of volume underestimation respectively). On the other hand the variability was greater for volume measurements performed on T2w images. Sagittal images were selected due to the familiarity of the observers with the anatomy of the foot when shown in this plane and due to the ability to visualise the entire extent of the NB. After a precise description of the anatomical landmarks it was estimated that 20 measurements were an appropriate number in order to train observers new to the technique. After training, measurement of NB volume could be performed in 5 minutes.

When intra- and inter-observer precision and accuracy were calculated (Chapter 3) sagittal T2w images were preferred over STIR images due to their improved performance. These findings correlate with the conclusions of a previous study conducted in human medicine where T2w images were considered adequate to assess the effusion of synovial structures (Loeuille *et al* 2011). The use of cadaver limbs was chosen for the validation of the method. This approach was preferred over the use of a phantom (Li *et al* 2010) because it was believed to replicate better naturally occurring disease (navicular bursitis). The measurements of NB volume made by a single observer (intra-observer experiment, *ex-vivo* study) indicated that overall accuracy was -40% of the volume injected (when 500-6000 mm^3 measurements are included) and -27% (when 500-3000 mm^3 measurements are included). These results compare favourably with value of 67% obtained during the validation studies carried out in human medicine using a semi-automated MRI system (Li *et al* 2010). In human medicine an accuracy of 20% was considered appropriate for MRI based methods of synovial volume measurement to be used in clinical cases (Ostergaard *et al* 1995). A similar value was obtained in the current study when volumes equal or lower than 3000 mm^3

were measured. It has previously been reported that the NB volume is approximately 3000mm^3 (Turner 1998). However, the volume of synovial fluid already present in the NB was not considered. It has also been reported that the NB is an elastic structure and can accommodate up to 6000 mm^3 before leakage is noted (Maher *et al* 2011). Injection of a volume of 10000 mm^3 has resulted in rupture of the NB (Schramme *et al* 2009). The great range of volume reported in the literature suggests that the NB is an elastic structure that can accommodate biologically irrelevant (i.e. higher that possible in physiological conditions) volumes of fluids. During the clinical part of this study (Chapter 5) only 7 measurements out of 20 were above 3000 mm^3. In five of these cases the volume measured was between 3000 and 4000 mm^3. These results suggest that the use of 3D Slicer® is appropriate in clinical cases.

Overestimation of the NB volume was noted in only 4 out of 144 measurements carried out in the intra-observer part of the study. All these measurements were for volumes equal or lower than 1500 mm^3. The close relationship of different anatomical structures resulting in reduced NB delineation was considered to be the main factor in this result (Maher *et al* 2011) athough others, including observer variability, leakage around needle tract and volume averaging artefact, could have contributed to NB volume underestimation. Volume averaging and operator error are considered to be constant throughout the study. Therefore the high frequency of underestimation of NB volume (negative values for accuracy using the method described here) was likely to be mainly the result of leakage of the water injected. This is supported by the increase in underestimation with the increase in volume of the NB (and therefore intra-luminal pressure). Accuracy of the method is likely to be improved in clinical cases where insertion of a needle in the NB is not required.

Overestimation was a general feature for the measurements of NB volume made by three different observers: A, B and C (inter-observer experiment, *ex-vivo* study Chapter 3). Overestimation was greater for observer “A”. When all the observers were included the median accuracy was 54% of the volume injected (i.e. 540 mm^3 of overestimation for each 1000 mm^3 injected). When observer “A” was excluded from the analysis the median accuracy for observers “B” and “C” was 32% (i.e. 540 mm^3 of overestimation for each 1000 mm^3 injected). All the volume measurements performed in the inter-observer part of the study were for volumes equal or lower to 2500 mm^3. As already noted for the intra-observer part of the

study the overestimation could be the result of close relationship of different synovial structures with similar signal intensity (Maher *et al* 2011). Furthermore, the use of a different region of interest (ROI) could have led to selection of a greater area leading to an overestimation as high as 20-30% (Cimmino *et al* 2003). The marked variation in performance between observers suggests that improved training and guidance in relation to image display parameters (ROI and windowing) prior to volume measurement is warranted.

The experience obtained with the use of 3D Slicer® during the *ex-vivo* part of the study (Chapter 3) was applied during the management of a clinical case with a DDFT lesion (Chapter 4). The case was managed with a novel approach that involved MRI guided injection of a DDFT insertional lesion. 3D Slicer® was used to calculate the NB volume, DDFT lesion volume and depth of needle insertion to reach the DDFT lesion. The volume of the DDFT lesion measured using 3D Slicer® was 30% less than the volume injected. This discrepancy is most likely explained by several different factors: volume averaging artefact, observer error during selection of the area to be measured, selection of the correct intensity signal but also core lesion expansion as a result of increased pressure during platelet rich plasma (PRP) injection. Most of the factors likely to be responsible for the underestimation identified in this chapter are similar to those identified in Chapter 3. It is interesting to note that although the volumes in the two chapters were different the accuracy appears to be similar (-30%) to the accuracy obtained in the intra-observer study (-27%).

The use of 3D Slicer® in clinical cases was explored in Chapter 5 where the objective method of NB volume measurement was compared to the current ‘gold standard’ (i.e. subjective assessment by a board certified radiologist). The results indicated that subjective assessment is a valid method to discriminate between horses with normal or mild effusion and cases with severe effusion. However, there was no significant difference in volume between bursae assessed as having normal or mild effusion, or moderate effusion and all other categories. These results suggest that a review of the subjective assessment criteria of NB effusion in clinical cases is warranted.

A cut-off value of 1768 mm^3 was 90% sensitive and specific in distinguishing between normal/mild and moderate/severe effusion. Reducing the number of

categories of NB effusion to normal and effused (abnormal) would reduce the apparent error rate of subjective assessment given that discrimination between normal, mild and moderate effusion appears particularly challenging. This change however can only be recommended if supported by the results of a larger scale study. Use of the anatomical landmarks for the NB and signal intensity description developed in Chapter 2 could be helpful in subjective assessment of NB volume, and may improve its performance.

The presence deep digital flexor tendon (DDFT) pathology was more likely to be diagnosed concurrently with severe NB effusion than other categories of effusion. All the cases belonging to the mild and moderate NB effusion were diagnosed with navicular syndrome. The presence of NB effusion in cases of navicular disease is thought to be related to degeneration of fibrocartilage on the flexor surface of the navicular bone. Fibrocartilage damage is one of the first signs of pathologic changes affecting the navicular bone (navicular disease). This cannot always be identified using MRI due to the close relationship of the fibrocartilage and DDFT (Schramme *et al* 2009). However, the identification of NB effusion in low field MR images could indicate navicular bursitis secondary to fibrocartilage damage. This suspicion could be confirmed by acquisition of high field spoiled gradient echo sequences (Murray *et al* 2005) or MR bursography (Schramme *et al* 2009).

One of the objectives of the current study was to determine the normal volume of the NB. The statistical analysis performed did not identify a significant difference between normal, mild and moderate effusion. For this reason a larger number of cases is required in order to identify a statistically significant difference between the different groups and establish a ‘normal’ value for NB effusion.

Future studies should aim at including more observers in order to further assess the performance of NB volume measurement using 3D Slicer®. Observer training should also be implemented by providing guidelines to improve the consistency image display (i.e. windowing of the selected ROI). The performance of the method should also be assessed in a larger number of clinical cases to explore further whether there is a statistically significant difference in volume between horses assessed subjectively to have normal, mild and moderate NB effusion.

In conclusion, the preliminary work presented in this this thesis supports the use of 3D Slicer® to measure objectively NB volume from sagittal T2w MR images in the horse, and suggests that this method is superior to subjective assessment of volume. Objective measurement of NB volume may be helpful in indicating the presence of specific pathology (e.g. DDFT tear or fibrocartilage lesions), which may prompt further investigation and inform treatment and prognosis. Furthermore, the use of sequential measurement of synovial structures volume could be used to assess the response to the treatment as has been reported in human medicine (Gait *et al* 2016).

Future work could involve the assessment of the 3D slicer® on sequential MRI examinations over time to assess response to treatment.

Appendices

1. Abstract presentation at the 26th ECVS Annual Scientific Meeting 13-15th July in Edinburgh, Scotland.

AUTHORS: M. Marcatili, J. Marshall and L. Voute

TITLE: Accuracy and precision of equine navicular bursa volume measurement made from low field MRI datasets using 3D Slicer® software – an *ex-vivo* study.

ABSTRACT

Introduction: Effusion of synovial joints and bursae is considered a reaction of the structure to traumatic or degenerative processes (1). This study aimed to validate a MRI based method for measuring navicular bursa (NB) volume objectively.

Material and Methods: Four forelimbs were harvested from two adult Thoroughbred horses euthanised for reasons other than lameness. An MRI-compatible needle* was positioned in the NB and connected to a syringe. Water was injected in 500 mm^3 increments up to a total of 300 mm^3. Low field (0.31T^2) sagittal and transverse T2 and STIR images were acquired before and after each injection. Volume was measured using 3D Slicer®. Accuracy was calculated as mean difference between injected and measured volume; precision as standard deviation of mean difference between injected and measured volume. Correlation between injected and measured volume was determined using Pearson's correlation coefficient.

Results: Volumes measured from T2 and STIR images were significantly ($p<0.001$) correlated with injected volume ($r=0.992$ and $r=0.998$ respectively). Measurements acquired from T2 images had significantly greater accuracy than STIR images (-510 mm^3 vs. -840 mm^3l). Measurements acquired from T2 images had significantly lower precision than STIR images (290 mm^3 vs. 220 mm^3). Measurements on both sequences underestimated the volume injected.

Discussion/Conclusion: The change in navicular bursa volume measured using 3D Slicer® software was significantly correlated with the volume injected. Reasons for underestimation are: leakage, volume averaging; observer error; or more likely a combination of these factors. Calculation of inter-observer variation in measurement is required before using this method for objective measurement of NB volume clinically.

2. Abstract presentation at the BEVA congress in Birmingham 12-15th September 2018

AUTHORS: M. Marcatili, J. Marshall, A. McKnight and L. Voute

TITLE: Objective measurement of navicular bursa volume.

Background: Navicular bursa (NB) effusion can be related to pathology. An objective method for measuring NB volume would be useful diagnostically and for patient monitoring.

Objectives: To evaluate an approach to measuring NB effusion and to compare measurements from horses with different pathologies

Study design: Clinical case series

Methods: Twenty front feet MRI studies acquired using a low field MRI machine (0.31 T)[1] were evaluated by a board certified radiologist. NB effusion was classified as normal, mild, moderate or severe. NB volume was measured from sagittal T2 sequences using 3D Slicer® software. The ability of objective measurements (the "test") to discriminate between groups was analysed using receiver operating characteristic (ROC) curves. Results: Average volumes were 1322±387 mm^3, 1187±486 mm^3, 2636±1012 mm^3 and 3833±1569 mm^3 for normal, mild, moderate and severe cases. There was a significant difference in volume measured between normal or mild and severe effusion ($p<0.05$). There was no significant difference between moderate and all other groups. ROC analyses showed that for a cut off value of 1798 mm^3 the test was 80% sensitive and 100% specific to identify moderate effusion, a cut off value of 1767 mm^3 was 100% sensitive and specific for severe effusion. Four out of five horses with severe effusion had deep digital flexor tendon (DDFT) lesions.

Main limitations: Sample size and single reader

Conclusions: Measurement of NB volume using MRI and 3D Slicer® software consistently identified a difference between normal or mild effusion and severe NB effusion, and supports the subjective evaluation of clinical cases. Further investigation of the method to increase sample size and evaluate the guidelines for different grades of NB effusion is merited. Horses with DDFT injuries appear to have a greater NB effusion compared to horses with other lesions of the podotrochlear apparatus.

[1]O- Scan equine, Esaote S.p.a. Genoa, Italy.

[1]SOMATEX® Medical Technologies GmbH | Rheinstr.7d, 14513 Teltow, Deutschland
[2] Esaote Spa, Genova, Italy.

3. Consent form signed by the owners of the horses enrolled in the clinical study.

Weipers Centre
EQUINE HOSPITAL

Weipers Centre Equine Hospital
School of Veterinary Medicine
College of Medical, Veterinary and Life Sciences
University of Glasgow
Bearsden Road
Glasgow G61 1QH
Telephone: 0141 330 5999 Fax: 0141 330 6025
E-mail (for appointments): equine@vet.gla.ac.uk

CONSENT FORM

Attach label here or hand print details:		
Owner's name:	Animal's name:	Breed:
Case number:	Clinician:	
Referring veterinarian:		

- I, the owner or agent of the above animal, hereby request that this animal receives such examination and treatment as may be required. This may include the administration of anaesthetic drugs, the act of surgery and treatment with drugs that may only be licensed for use in other species. The nature and effect of this examination and treatment have been explained to me.
- No assurance has been given that the treatment will be carried out by a particular veterinary surgeon. I understand that students, acting under appropriate supervision, may be involved in the examination and care of my animal.
- I give my permission for the retention and use of all clinical data/records, pictures (including digital diagnostic images), samples (urine, blood, DNA, biopsies, autopsies) for teaching purposes and for future studies to help animal welfare. All such material will be used anonymously.
- I, the owner or agent certify that the horse is not intended for human consumption.
- Any information that you supply via this form will be entered into a filing system and will only be accessed by authorised persons of the University of Glasgow or its agents. By supplying such information you consent to the University storing the information for the stated purposes. The information is processed by the University in accordance with the provisions of the Data Protection Act 1998.

Total current estimated cost: £……..… (excluding VAT)

- I also realise that the estimated costs of treatment can only be approximate and do not include any emergency procedures, follow up treatment or investigation. I accept that I am liable for all costs incurred in the treatment of my animal and agree to pay in full upon collection of my animal. I agree to the University's Terms and Conditions for the provision of services.

I agree ☐ **I disagree** ☐

Signed: …… Date:……

WITNESS: I confirm that I have explained to the owner or agent the nature and effects of the examination and treatment to be carried out on the above named animal.

Signed……..(MRCVS) Date:……

Please note: Visiting hours are between 4pm and 5.00pm weekdays, 11am-12noon on weekends; **only** by prior arrangement with the staff. Please report to reception when visiting.

- 4. MRI sequences technical parameters

Sequence	Echo time (TE)	Repetition time (TR)	Pixel size mm	Field of view (FOV) mm
T1	16	760	1	200
TMP PD-T2	28	3270	1	200
STIR	26	3200	1	200

List of references

- American Association of Equine Practitioners (1999): Guide to veterinary services for horse shows, ed 7, Lexington, KY.

- Arnoczky SP and Sheibani-Rad S (2013): The basic science of platelet rich plasma (PRP): what clinicians need to know. Sports Med Arthrosc, 21 (4). pp. 180-185.

- Barker WHJ, Smith MRW, Minshall GJ, Wright IM (2013): Soft tissue injuries of the tarsocrural joint: A retrospective analysis of 30 cases evaluated arthroscopically. Equine Veterinary Journal, 45. pp. 435–441.

- Blunden A, Dyson S, Murray R, Schramme M (2006): Histological findings in horses with chronic palmar foot pain and age-matched control horses. Part 1: the navicular bone and related structures. Equine Vet J, 38. pp. 15–22.

- Bolas (2011): Basic MRI principles. In: Murray: Equine MRI. First edition, Wiley-Blackwell, pp. 3-37.

- Busoni V and Denoix JM (2001): Ultrasonography of the podotrochlear apparatus in the horse using a transcuneal approach: technique and reference images. Veterinary Radiology & Ultrasound, 42. pp. 534–540.

- Busoni V, Heimann M, Trenteseaux J, Snaps F, Dondelinger RF (2005): Magnetic resonance imaging findings in the equine deep digital flexor tendon and distal sesamoid bone in advanced navicular disease-an ex vivo study. Veterinary Radiology Ultrasound, 46. pp. 279–286.

- Carstens A and Smith RKW (2014): Ultrasonography of the foot and pastern. In: Atlas of equine ultrasonography. Kidd JA, Lu KG and Frazer ML. First edition. Wiley Blackwell. pp. 25-44.

- Cimmino MA, Innocenti S, Livrone F, Magnaguagno F, Silvestri E, Garlaschi G (2003): Dynamic gadolinium-enhanced magnetic resonance

imaging of the wrist in patients with rheumatoid arthritis can discriminate active from inactive disease. Arthritis and Rheumatism, 48, no. 5, pp. 1207–1213.

- Coelho and Kinns (2012): Magnetic resonance imaging. In: Auer and Stick. Equine surgery. Auer JA and Stick JA. Elsevier Saunders 4th edition. pp. 985-997.

- Delecrin J and Oka M (1992): Measurement of synovial fluid volume: a new dilution method adapted to fluid permeation from the synovial cavity. J Rheumatol, 34. pp. 1746–1752.

- Dyson S, Blunden T, Murray R (2012): Comparison between magnetic resonance imaging and histological findings in the navicular bone of horses with foot pain. Equine Veterinary Journal, 44. pp. 692–698.

- Dyson S, Murray R, Blunden T, Schramme M (2006): Current concepts of navicular disease. Equine Vet Educ, 18. pp. 45–56.

- Dyson S, Murray R, Schramme M (2005): Lameness associated with foot pain: results of 199 horses (January 2001–December 2003) and response to treatment. Equine Vet J, 37. pp. 113–21.

- Dyson SJ, Murray R, Schramme, Blunden T (2011): Current concept of navicular disease. Equine Vet Educ, 23. pp. 27–38.

- Egger J, Kapur T, Fedorov A, Pieper S, Miller J V, Veeraraghavan H, Freisleben B, Golby AJ, Nimsky C, Kikinis R (2013): GBM volumetry using the 3D Slicer medical image computing platform. Sci Rep, 3:1364, pp 1-7.

- Ekman L, Nilsson G, Persson L,Lumsden JH (1981): Volume of the synovia in certain joint cavities in the horse. Acta Vet Scand, 22 (1). pp. 23-31.

- Geborek P, Saxne T, Heinegard D, Wollheim FA (1988): Measurement of synovial fluid volume using albumin dilution upon intraarticular saline injection. J Rheumatol, 15. pp. 91–94.

- Gough MR, Munroe GA and Mayhew IG (2006) Urea as a measure of dilution of equine synovial fluid. Equine Veterinary Journal, 34. pp 1–4.

- Groom LM, White NA, Adams MN, Barrett JG (2017): Accuracy of open magnetic resonance imaging for guiding injection of the equine deep digital flexor tendon within the hoof. Veterinary Radiology & Ultrasound, 58. pp. 671–678.

- Heuck AF, Steiger P, Stoller DW, Gluer CC, Genant HK (1989): Quantification of knee joint fluid volume by MR imaging and CT using three-dimensional data processing. J Comput Assist Tomogr, 13. pp. 287-293.

- Jennings D, Fennessy F, Sonka M, Buatti J (2013): 3D Slicer as an Image Computing Platform for the Quantitative Imaging Network. Magn Reson Imaging, 30. pp. 1323–1341.

- Kane-Smith J, Taylor SE, Cillan Garcia E and Reardon JM (2016): Frequency of penetration of the digital flexor tendon sheath and distal interphalangeal joint using a direct endoscopic approach to the navicular bursa in horses. Veterinary surgery, 45, pp. 380-385.

- Kraus VB, Stabler TV, Kong J, Varju G and McDaniel G (2007): Measurement of Synovial Fluid Volume Using Urea, Osteoarthritis Cartilage, 15(10). pp. 1217–1220.

- Lamb MM, Barrett JG, White NA, II, Were SR (2014): Accuracy of low-field magnetic resonance imaging versus radiography for guiding injection of equine distal interphalangeal joint collateral ligaments. Veterinary Radiology & Ultrasound, 55. pp. 174–181.

- Li W, Abram F, Pelletier JP, Raynauld JP, Dorias M, d'Anjou MA, Martel-Pelletier J (2010): Fully automated system for the quantification of human osteoarthritic knee joint effusion volume using magnetic resonance imaging. Arthritis Res & Therapy, 12:R173.

- Loeuille D, Sauliere N, Champigneulle J, Rat AC, Blum A, Chary-Valckenaere I (2011): Comparing non-enhanced and enhanced sequences in the assessment of effusion and synovitis in knee OA: associations with clinical, macroscopic and microscopic features. Osteoarthritis and Cartilage, 19(12). pp. 1433–1439.

- Ma Z, Chen X, Huang Y, He L, Liang C, Liang C, Liu Z (2015): MR diffusion-weighted imaging-based subcutaneous tumour volumetry in a xenografted nude mouse model using 3D Slicer: an accurate and repeatable method. Sci. Rep. 5, 15653.

- Maher MC, Werpy NM, Goodrich LR, McIlwraith CW (2011): Positive contrast magnetic resonance bursography for assessment of the navicular bursa and surrounding soft tissues. Veterinary Radiology & Ultrasound 52. pp. 385–393.

- Matsuzaka S, Sato S, Miyauchi S (2002): Estimation of joint fluid volume in the knee joint of rabbits by measuring the endogenous calcium concentration. Clin Exp Rheumatol, 20. pp. 531–534.

- McIlwraith CW, Nixon AJ and Wright IM (2015): Bursoscopy. In: McIlwraith CW, Nixon AJ and Wright IM: Diagnostic and surgical arthroscopy in the horse. Fourth edition. Mosby Elsevier. pp. 387-406.

- Mercea P (1985): Quantification of longitudinal tumor changes using PET imaging in 3D Slicer. Master Thesis. Ruperto Carola University of Heidelberg, Germany.

- Murray R and Werpy N (2011): Image interpretation and artefacts. In: Equine MRI. First edition. Wiley- Blackwell. pp. 101–145.

- Murray R, Schramme M, Dyson S, Branch M, Blunden A (2006): MRI characteristics of the foot in horses with palmar foot pain and control horses. Vet Radiol Ultrasound, 47. pp. 1–16.

- Murray RC, Branch MV, Tranquille C, Woods S (2005): Validation of magnetic resonance imaging for measurement of equine articular cartilage and subchondral bone thickness. Am J Vet Res, 66. pp.1999–2005.

- Nelson BB, Goodrich LR, Barrett MF, Grinstaff MW, Kawcak CE (2017): Use of contrast media in computed tomography and magnetic resonance imaging in horses: Techniques, adverse events and opportunities. Equine Veterinary Journal, 49. pp. 410–424.

- O'Neill TW, Parkes MJ, Maricar N, Marjanovic EJ, Hodgson R, Gait AD, Cootes TF, Hutchinson CE, Felson DT (2016): Synovial tissue volume: a treatment target in knee osteoarthritis (OA). Annals of the Rheumatic Diseases, 75(1). pp. 84–90.

- Ostergaard M, Gideon P, Henriksen O, Lorenzen I (1994): Synovial volume: a marker of disease severity in rheumatoid arthritis? Quantification by MRI. Scand J Rheumatol, 23. pp. 197-202.

- Ostergaard M, Stoltenberg M, Gideon P, Sorensen K, Henriksen O, Lorenzen I (1996): Changes in synovial membrane and joint effusion volumes after intraarticular methylprednisolone: quantitative assessment of inflammatory and destructive changes in arthritis by MRI. J Rheumatol, 23. pp. 1151-1161.

- Ostergaard M, Stoltenberg M, Henriksen O, Lorenzen I (1995): The accuracy of MRI-determined synovial membrane and joint effusion volumes in arthritis: a comparison of pre- and post-aspiration volumes. Scand J Rheumatol, 24. pp. 305-311.

- Peterfy CG, Guermazi A, Zaim S, Tirman PF, Miaux Y, White D, Kothari M, Lu Y, Fye K, Zhao S, Genant HK (2004): Whole-Organ Magnetic Resonance Imaging Score (WORMS) of the knee in osteoarthritis. Osteoarthritis Cartilage, 12. pp. 177-90.

- Pieper S, Lorensen B, Schroeder W, Kikinis R (2007): The NA-MIC Kit: ITK, VTK, Pipelines, Grids and 3D Slicer as An Open Platform for the Medical Image Computing Community. J Digit Imaging. pp. 698–701.

- Prior A and Marshall JF (2014): 3D Slicer and its ability to function as a Diagnostic Tool in the Veterinary field. University of Glasgow.

- Rekonen A, Oka M, Kuikka J (1973): Measurement of synovial fluid volume by a radioisotope method. Scand J Rheumatol, 2. pp. 33-35.

- Ross MW (2011): Lameness in horses: Basic facts before starting. In: Diagnosis and management of lameness in the horse. Ross MW and Dyson SJ. Second Edition. Elsevier Saunders. pp. 3-7.

- Ross MW (2011): Observation: symmetry and posture. In: Diagnosis and management of lameness in the horse. Ross MW and Dyson SJ. Second Edition. Elsevier Saunders. pp. 32-42.

- Sampson SN, Schneider RK, Gavin PR, Ho CP, Tucker RL, Charles EM (2009): Magnetic resonance imaging findings in horses with recent onset navicular syndrome but without radiographic abnormalities. Veterinary Radiology & Ultrasound, 50(4). pp. 339–346.

- Schramme M, Kerekes Z, Hunter S, Nagy K, Pease A (2009): Improved identification of the palmar fibrocartilage of the navicular bone with saline magnetic resonance bursography. Veterinary radiology & ultrasound, 50. pp. 606–614.

- Schramme MC, Boswell JC, Hamhougias K, Toulson K and Viitanen, M. (2006): An in vitro study to compare 5 different techniques for injection of the navicular bursa in the horse. Equine Vet J, 32 (3). pp. 263-267.

- Sequeiros RB, Ojala R, Kariniemi J, Perälä J, Niinimäki J, Reinikainen H, Tervonen O (2005): MR-Guided Interventional Procedures: A Review, Acta Radiologica, 46:6. pp. 576-586.

- Smith MRW, Wright IM (2012): Endoscopic evaluation of the navicular bursa; observations, treatment and outcome in 93 cases with identified pathology. Equine Vet J, 44. pp. 339-345.

- Smith MRW, Wright IM, Smith RKW (2007): Endoscopic assessment and treatment of lesions of the deep digital flexor tendon in the navicular bursae of 20 lame horses, Equine Vet J, 39. pp. 18-24.

- Svalastoga E, Neilsen K (1983): Navicular disease in the horse: the synovial membrane of bursa podotrochlearis. Nord Vet Med, 35. pp. 28-30.

- Tevik A (1983): The role of anesthesia in surgical mortality in horses. Nord Vet Med, 35. pp. 175-179.

- Turner TA (1998): Use of navicular bursography in 97 horses, in *Proceedings.* 42nd Annu Conv Am Assoc Equine Practnr, 44. pp. 227-229.

- Vallance SA, Bell RJW, Spriet M, Kass PH, Puchalski S.M (2011): Comparisons of computed tomography, contrast enhanced computed tomography and standing low-field magnetic resonance imaging in horses with lameness localised to the foot. Part 1: Anatomic visualisation scores. Equine Veterinary Journal, 44. pp. 51–56.

- van Hamel SE, Bergman HJ, Puchalski SM, de Groot MW, van Weeren PR (2013): Contrast-enhanced computed tomographic evaluation of the deep digital flexor tendon in the equine foot compared to macroscopic and histological findings in 23 limbs. Equine Veterinary Journal. 46, pp. 300–305.

- Widmer WR, Buckwalter KA, Fessler JF (2000): The use of radiography, computed tomography and magnetic resonance imaging for evaluation of navicular syndrome in the horse. Vet Radiol Ultrasound, 41. pp. 108-116.

- Wolff J, Gu H, Gerig G (2012): Differences in white matter fiber tract development present from 6 to 24 months in infants with autism. Am J Psychiatry, 169. pp. 589–600.

- Wright IM, Phillips TJ and Walmsley JP (1999): Endoscopy of the navicular bursa: a new technique for the treatment of contaminated septic bursae. Equine Veterinary Journal, 31. pp. 5-11.

- Young SS and Taylor PM (1990): The effect of limb position on venous and compartmental pressure in the forelimb of ponies. Vet Anaesth Analg, 17. pp. 35-37.

Word count: 23255